Radboud University Nijmegen

Faculty of Science

Tree bijections in Two-Dimensional Quantum Gravity

Distance Statistics from Tree bijections of Regular and Eulerian Quadrangulations

Thesis BSc Physics and Astronomy

Author:
Jan Groenendijk

Supervisor:
dr. Timothy Budd

Second reader:
dr. Ross Kang

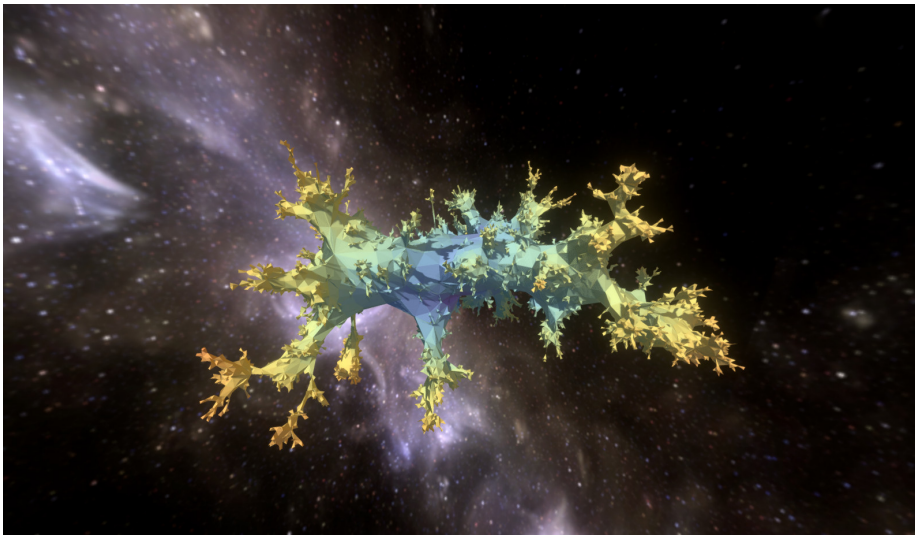

June 2021

Acknowledgements

Over the course of my bachelor's degree, I have developed a strong interest in two different subjects within my studies - relativity theory and particle physics. Unfortunately, said studies does *not* contain a course on merging quantum mechanics and general relativity - which is logical, because it is still very much an open problem in modern physics. However, it did contain a course on *special* relativistic quantum mechanics and - coincidentally - Dr. Timothy Budd was my teacher for this course. It is only fitting that I am now ending my bachelor with a thesis on quantum gravity, under his supervision. I wish to thank Mr. Budd for many interesting ideas and discussions, on approximately any topic that the reader will encounter in this thesis. [1]

[1] Titlepage image credit: dr. Timothy Budd.

Contents

1 Introduction

Through the past decades, formulating a consistent theory of Quantum Gravity where one tries to combine the fundamental laws of quantum mechanics and Einstein's theory of relativity, has become a very well studied open problem in physics. There are currently many different approaches that are being taken to tackle this problem. According to Einstein's theory of general relativity a change in the energy density content of a spacetime will result in a change of the metric of said spacetime, and hence, *gravity* can be viewed as a purely geometrical feature. It does a stellar job in explaining the dynamics of planets, stars, galaxies, and even the time evolution of the universe as a whole, as seen in figure 1. Contrary to the typical length scales of general relativity, quantum me-

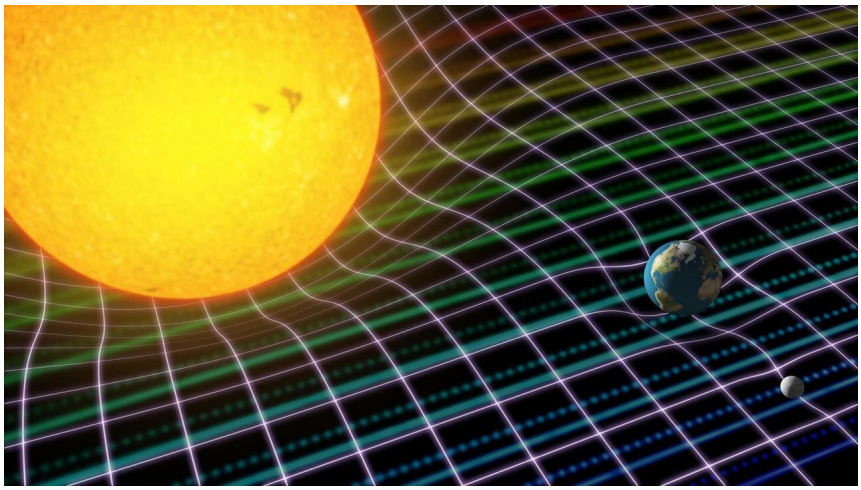

Figure 1: General Relativity made visible. Image credit: phys.org

chanics describes the dynamics of the smallest possible particles. As the name suggests, an important feature of quantum mechanics is that some things that seem continuous - e.g. energy spectra - are actually, and surprisingly, quantized. Quantum mechanics is often formulated using the *path integral formalism*, where one computes an infinite dimensional integral over all possible paths from point A to point B, of an appropriate weight depending on the action over the considered path. The path that the particle may take, is in essence *random*.

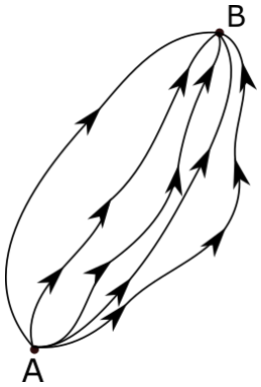

Figure 2: The path integral formalism of Quantum Mechanics. Image credit: wikipedia.

In combining these fundamental aspects of Quantum Mechanics and General Relativity, to obtain a suitable theory of Quantum Gravity, one must compute an infinite dimensional integral over all possible geometries of four-dimensional spacetime, weighted by the Einstein-Hilbert action. One way to look at this is by taking into account the 'random' part of quantum mechanics, and the 'geometry' part of General Relativity: *random geometry*. What this means is that we may study the integral over all geometries of spacetime by discretizing these geometries: we take n identical building blocks, and look at the limit where this number of building blocks approaches infinity. One of the largest advantages of this approach, is that properties of discrete models are much easier to analyse. We may extract exact relations for geometries obtained from n identical building blocks, and study their asymptotic behaviour in the large n limit.
Doing this for four-dimensional geometries might be the key to a consistent theory of quantum gravity. However, this turns out to be quite a challenge. Therefore, this research focuses on a simplified model of random geometry in two dimensions instead of four, in the absence of matter. In this case, the *weight* that a geometry obtains from the Einstein-Hilbert action is constant, and therefore all the different geometries obtain an equal probability.

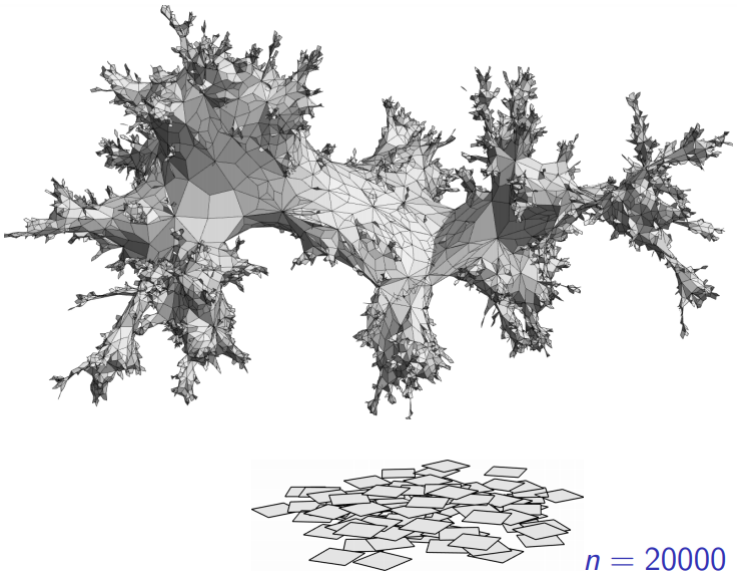

Figure 3: The random geometry obtained by gluing together two-dimensional quadrangles, in the large n limit. Image credit: dr. Timothy Budd.

In this research we will study the geometries obtained from the specific case of quadrangles cut out of the Euclidian plane, as seen in figure 3, where every 'enclosed area' is bounded by four edges and four vertices (or points). But firstly, and more importantly, what I would like to point out is that essentially the discrete structure of the building blocks of the geometry does not matter - albeit triangles, quadrangles, or higher order polygons - up to a constant rescaling (which *does* depend on the discrete building blocks) the limit

$$\lim_{n\to\infty} \left(V(M_n), c_p\, n^{-1/4} d_{gr} \right) = (m_\infty, d_\infty) \tag{1}$$

is the same for all regular p-gons that we can cut out of the plane! The set of 'points' $V(M_n)$ of our discrete geometry, equipped with a distance function $f(x,y) = c_p\, n^{-1/4} d_{gr}(x,y)$ where $d_{gr}(x,y)$ is the geodesic *graph distance* between the points x and y, converges in

distribution to a well-defined random metric space (m_∞, d_∞) in the Gromov-Hausdorff topology (whose definition goes beyond the scope of this thesis) [10]. This limit is called the *Brownian Map*. Perhaps the most important thing is, that we can always choose the constant c_p such that the limit is truly independent(!) of the discrete nature of our building blocks, for all p. By comparing figure 3 and figure 4, one may see that these two discrete geometries might indeed coincide in the large n limit.
This means, most importantly, that the Brownian Map carries a certain universality: apparently, it is the universal limit for geometries made out of a large number of identical building blocks, but perhaps it is the universal limit for other kinds of two-dimensional maps as well.

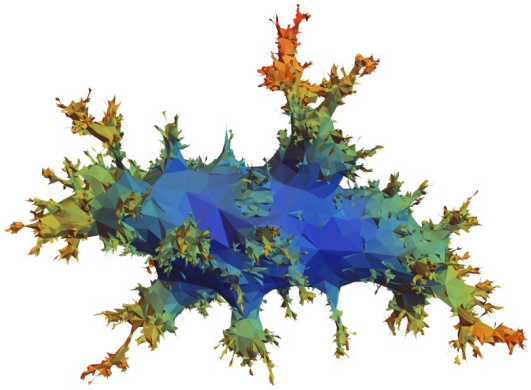

Figure 4: A gluing of two dimensional triangular shapes. From this image is clearly visible that, in the large n limit, the quadrangulation of figure 3 and this triangulation might coincide. Image credit: dr. Timothy Budd.

The geometry of the Brownian Map comes with some surprising properties. For a start, one would expect a typical distance within a two-dimensional surface to scale with the square root of the area of said surface. However, within the Brownian Map, one of the striking features is that typical distances in the limiting random geometry scale with the fourth root(!) of the area. This is readily seen by the rescaling of the graph distances in equation (1) by this exact factor of $n^{-1/4}$. It has been established that this is indeed the unique rescaling that one needs for the convergence of (1).
Another way of saying that geodesic distances scale with the fourth root of the total volume, is by saying that the *Hausdorff dimension* of the surface is equal to 4. A surface whose Hausdorff dimension is unequal to 2, is considered 'fractal'. This implies that the properties of the geometry are essentially *scale-invariant*. Actually, this is precisely what we are looking for in a model of two-dimensional quantum gravity without matter. One of the biggest problems is that 'naive' quantizations of the geometry of spacetime break down when considered on quantum mechanical length scales, close to the Planck scale. One possible solution for two-dimensional quantum gravity is indeed by consdering purely fractal surfaces, such that the geometrical properties of the spacetime are invariant under 'zooming' beyond the Planck scale!
In this research, I will be aiming to recover this specific dimensional feature of distance rescaling by $n^{-1/4}$, by means of two mathematical models using bijections with trees; the first of which is already quite well and thoroughly understood, and the second one is not (as much).
Firstly, we will take a look at a bijection between normal or *regular* quadrangulations and a certain class of trees, *well-labelled trees*, and investigate how properties on the

quadrangulations translate to properties on the corresponding trees, which are easier to analyse. Specifically, the fourth root feature will be recovered in two ways - one using the properties of the labelling of the trees they inherit from the bijection, and a more precise derivation using the asymptotic features of the generating functions of these well-labelled trees in the limit where the number of building blocks becomes large.
Secondly - since one of my greatest interests besides physics (and mathematics, for that matter) is the wonderful game of 10 x 10 draughts, I will be looking at *Eulerian Quadrangulations*, which are black and white colored quadrangulations of the plane such that all white squares must be adjacent to black squares and vice versa. In this different class of maps I will be investigating a bijection with yet another class of trees - so called *labelled mobiles* - and aim to recover the same fourth root feature as in the previous model. This will be done by setting up a recurrence relation for their generating functions and studying their asymptotics by comparing them to regular quadrangulations.
In doing so, I hope to recover the same distance scaling of $n^{1/4}$ as for the regular quadrangulations, which would be a strong indication that Eulerian quadrangulations are within the universality of the Brownian Map as well.

2 Introduction to Maps and Generating Functions

To start off, it might be useful to quickly go through some definitions of mathematical objects that will be of great importance throughout this thesis. Even though there are many interesting things to say about these objects and interesting theorems to point out, I will try to stick to what is really necessary as much as I can.

2.1 Maps

The start of this chapter will be on graphs, maps, and a wonderful theorem by Leonhard Euler.

Definition 2.1. A *graph* is a finite set of *vertices* (points), *edges* (lines) and an *incidence mapping* that connects pairs of vertices by an edge.

In this definition, it is also allowed to have loops or cycles within the graph (e.g. a loop is obtained by setting the two vertices that an edge connects equal to each other), or vertices that exist by themselves without an edge binding to them. Let us define the following:

Definition 2.2. A *connected* graph is a graph that has no disconnected vertices; between any two vertices in the graph, there exists a path connecting them.

The *degree* of a vertex is the number of edges incident to it.
The following definition is straightforward, but I want to give it the attention it deserves, because it is indeed quite important.

Definition 2.3. A *tree* is a connected graph that contains no loops or cycles. Equivalently, a tree is a connected graph that would become disconnected by the removal of any one of its edges.

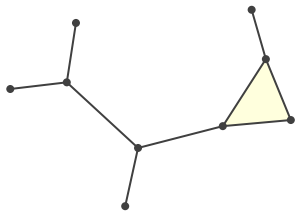

Figure 5: A connected graph, but *not* a tree.

Graphs and trees can be *rooted*; this corresponds to marking a specific vertex to be the root of the graph. In the case of a tree, we will often call the tree *planted* if it has a such a root.
Let us now turn to the definition of a map.

Definition 2.4. A *surface* is a closed, connected two-dimensional manifold. Any surface of genus g is *homeomorphic* with the sphere with g handles attached.

I'm not going to go into too much detail here on the genus of a surface and homeomorphisms, since we will only be considering surfaces of genus 0. In essence, the genus of a surface can be thought of as the number of distinct holes it has, and a homeomorphism between two surfaces can be thought of as a continuous deformation of one surface into the other.

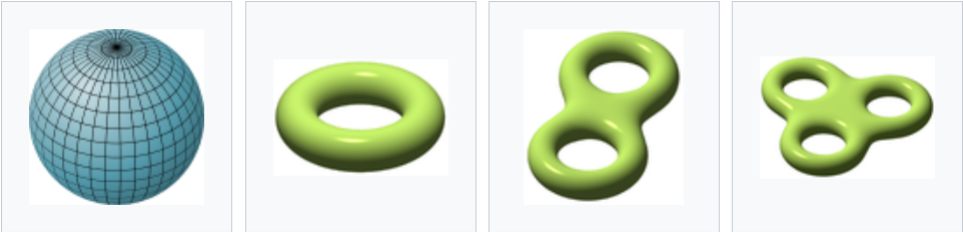

Figure 6: Surfaces of genus 0, 1, 2 and 3 respectively. Image credit: wikipedia.

Definition 2.5. An *embedding* of a connected graph G into a surface S is a drawing of the graph on the surface such that:

- each vertex of the graph is represented by a point in S and distinct vertices are represented by distinct points;
- each edge of the graph is represented by a non-selfintersecting curvilinear segment in S, with the ends of the segment coinciding with the vertices connected by the edge. No two segments intersect;
- The complement to the image of G in S is a *disjoint* union of two-dimensional domains homeomorphic to disks.

The image of a graph under such an embedding is called a *map*. Two maps are considered equivalent if there exists an *orientation preserving homeomorphism* of the plane taking the image of the first embedding into the second one. The connected components of $S \backslash G$ are called the *faces* of the map. The *degree* of a face is the number of edges it is bounded by.
Maps, as well as graphs, can be rooted. In this case, this corresponds to marking a specific edge on the map with an orientation.

Remark. Any graph G embedded in a surface S has a so called *dual map*, which is the graph embedded into S whose vertices and edges are in one-to-one correspondence with the faces and edges of G respectively, and each edge of the dual map connects the vertices corresponding to the faces separated by the corresponding edge of G.

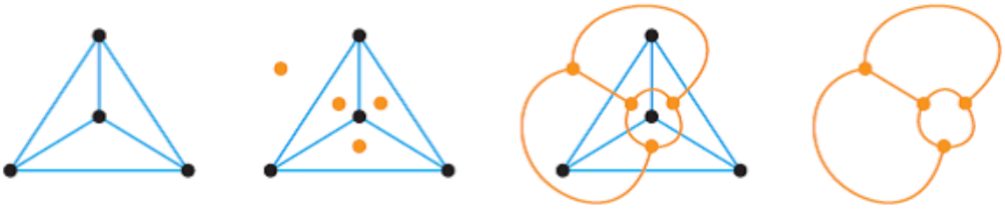

Figure 7: A graph, and the construction of its dual graph. Image credit: chegg.com.

Now that all of this is settled, we can finally state Euler's formula.

Theorem 2.6. ***Euler's theorem.*** *For a map of genus g with n edges, f faces and v vertices, the following relation holds:*

$$v + f - e = 2 - 2g \tag{2}$$

This is an amazingly simple relation between the numbers of vertices, faces and edges of a map and the genus of the surface it is embedded in. In the literature, the quantity $2-2g$ is sometimes also being named the *Euler characteristic* of the surface.
Since we will actually only be considering *planar* graphs, i.e. graphs with zero genus, the relation reduces to $v+f-e=2$ in our case. I think it is safe to say that proving the formula for surfaces of arbitrary genus is still quite challenging, but in our zero genus case it is somehow intuitive that it works - any edge must connect two vertices, and adding a vertex means automatically adding an edge, whether the vertex is placed in the middle of an already existing edge, or elsewhere. Furthermore, the same argument can be made for the faces; a face can be divided into two faces by adding an edge, so in the same way as between the edges and vertices, there is some kind of a balance between the number of edges and the number of faces of a map.
Of course, this was not an official proof of the theorem, but it does give some insight as to why the relations holds - which for the purpose of this thesis should be enough. An interested reader may find more on Euler's theorem in [13].

Definition 2.7. A *planar* map is a graph embedded into a genus zero surface. It can be represented in the plane by sending the 'outer' face to infinity. Every planar map also has a spherical representation, which maps the infinite outer face of the planar map onto a finite face within the sphere.

This thesis will be on unicolored and bicolored quadrangulations of the plane. To that end, let us define:

Definition 2.8. A *planar quadrangulation* is a graph embedded in the plane in which all faces have degree four.

Furthermore, a tree can also be thought of as a *one-face map of genus zero*. By Euler's formula, a tree with n vertices has $n-1$ edges - as it should. An equivalence class of embeddings of a tree in the plane is called a *plane tree*.

2.2 Generating Functions

We can very nicely study maps (and trees specifically) via their *generating functions*. This might come in handy for e.g. the enumeration of maps, as we will see shortly - but later on, it proves to be very useful in defining recursive sequences for certain classes of trees as well. Generating functions provide a rather intuitive way to convert 'counting problems' of certain combinatorial objects into algebraic problems of the corresponding generating functions.

Definition 2.9. The *generating function* of a sequence of numbers $a_0, a_1, a_2, ...$ is the power series $G(x)=\sum_{n=0}^{\infty} a_n x^n$.

More often than not, this is to be considered as a *formal* power series; this means that we do not really wish to evaluate the function $G(x)$ at some value of x, but that we are merely converting a 'counting' problem into an algebraic problem on the corresponding generating functions. These functions are in general much easier to manipulate. For example, the generating function of *triples* of some combinatorial object defined by the function $G(x)$, is equal to $G(x)^3$.
We may use this formalism to calculate the number of planted plane trees with a given number of edges, by manipulating their generating functions. Let us provocatively denote the sequence of the number of plane trees with $n=0,1,2,3,...$ edges by C_n. These numbers are called the *Catalan numbers* and have a whole range of applications in different combinatorial fields. To start our quest, let us define what is called a regular bracket structure:

Definition 2.10. A *regular bracket structure* is a sequence of opening and closing brackets, such that:

- there are as many opening as closing brackets;
- at any point in reading the sequence from left to right, the number of closing brackets cannot exceed the number of opening brackets;
- upon removing any opening bracket and its 'associated' closing bracket, the remaining sequence must still be a regular bracket structure.

For example, the sequence (((())())() is regular; the sequence (()())(()))(is not.
The number of planted plane trees with n edges is precisely equal to the number of *regular bracket structures* with $2n$ brackets. This is seen by considering a walk along the contour of a planted tree, starting from the root. Such a contour walk traverses every edge precisely two times, once away from the root vertex and once towards the root vertex. We associate a step 'away' from the root with an opening bracket and a step towards the root with a closing bracket. After $2n$ steps, we return to the root vertex, and by construction we have obtained a regular bracket structure. See figure 8.
Using the regular bracket structures, we can write down a recursion relation for the

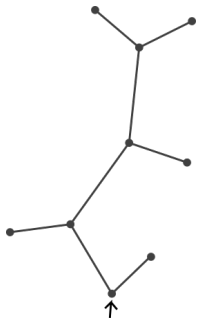

Figure 8: The plane tree corresponding to the bracket structure (()((()())()))().

Catalan numbers [9]. The number of ways one can organize 2(n+1) brackets, denoted by C_{n+1}, is, in terms of the previous Catalan numbers $C_n, C_{n-1}, C_{n-2}, ..., C_0$ given by

$$C_{n+1} = C_0C_n + C_1C_{n-1} + ... + C_{n-1}C_1 + C_nC_0 = \sum_{k=0}^{n} C_kC_{n-k}. \tag{3}$$

This is seen by noting that any regular bracket structure can be decomposed in terms of two regular structures as $(X)Y$, where we allow either X or Y to be empty. Next we count all possible configurations where X has k pairs and Y has $n-k$ pairs in total, for all possible $k \in [0, n]$. Adding them up, we find the total number of bracket structures with $n+1$ brackets.
Next, we denote the generating function of the Catalan numbers to be $C(x) = \sum_{n=0}^{\infty} C_n x^n$. Then, by the previous observation, we find that

$$\sum_{n=0}^{\infty} C_{n+1}x^n = \sum_{n=0}^{\infty} \left(\sum_{k=0}^{n} C_kC_{n-k} \right) x^n = \sum_{k=0}^{\infty} C_k x^k \sum_{n=k}^{\infty} C_{n-k}x^{n-k} \tag{4}$$

$$= \sum_{k=0}^{\infty} C_k x^k \sum_{l=0}^{\infty} C_l x^l = C^2(x), \tag{5}$$

where the substitution $n = k + l$ was made in going from the first line to the second line. We find

$$\frac{1}{x}\sum_{n=0}^{\infty} C_{n+1}x^{n+1} = C^2(x), \tag{6}$$

and we can further simplify this by writing

$$\frac{1}{x}\left(\sum_{n=0}^{\infty} C_n x^n - C_0\right) = C^2(x), \tag{7}$$

and since we know that $C_0 = 1$, we can obtain from this a quadratic equation in $C(x)$ given by

$$xC^2(x) - C(x) + 1 = 0, \tag{8}$$

and this is easily solved to be:

$$C(x) = \frac{1 \pm \sqrt{1-4x}}{2x}. \tag{9}$$

For the choice between the positive and the negative square root, it is sufficient to observe - once again - that $C(0) = C_0$ must evaluate to 1, which is clearly not the case for the positive square root. For the negative square root, we have a case of $\frac{0}{0}$, but the limit is straightforwardly computed to be 1. Therefore it is clear that $C(x) = \frac{1-\sqrt{1-4x}}{2x}$ is the function we are looking for. This is the well-known generating function for the Catalan numbers.
The enumeration of plane trees now follows from an interesting theorem.

Theorem 2.11. ***Lagrange's Inversion Formula****. Suppose two formal power series $G(x)$ with $G(0) = 0$, and $F(t)$ with $F(0) \neq 0$ are related by $G(x) = xF(G(x))$. Then for the coefficients of the function, we have the relation*

$$[x^n]G(x) = \frac{1}{n}[t^{n-1}]F^n(t), \tag{10}$$

where $[x^n]G(x)$ denotes the coefficient of x^n in the power series $G(x)$.

For a proof of this theorem, as well as interesting notes and alternate forms, I would like to refer to [12].
Unfortunately equation [8] is not yet in the right form for the above theorem to be applied, but we can make it that way. Let us set $G(x) = C(x) - 1$, and $F(t) = (1+t)^2$. The reader can check by themselves that upon doing these substitutions, the desired form $G(x) = xF(G(x)$ is automatically obtained! Let us now readily use the theorem and calculate the coefficients of $C(x)$.

$$\begin{aligned}
[x^n]G(x) &= \frac{1}{n}[t^{n-1}](F(t))^n \\
\implies [x^n]G(x) &= \frac{1}{n}[t^{n-1}](1+t)^{2n} \\
[x^n]G(x) &= \frac{1}{n}[t^{n-1}]\left(\sum_{k=0}^{2n}\binom{2n}{k}1^{2n-k}t^k\right) \\
[x^n]G(x) &= \frac{1}{n}\binom{2n}{n-1},
\end{aligned}$$

where we have used Newton's binomial formula to expand $(1+t)^{2n}$. Finally we find

$$[x^n]G(x) = \frac{1}{n+1}\binom{2n}{n}, \tag{11}$$

and hence the generating function for the Catalan numbers becomes

$$C(x) = \sum_{n=0}^{\infty} C_n x^n \tag{12}$$

$$= 1 + \sum_{n=1}^{\infty} \frac{1}{n+1} \binom{2n}{n} x^n \tag{13}$$

$$= \sum_{n=0}^{\infty} \frac{1}{n+1} \binom{2n}{n} x^n \tag{14}$$

- the coefficient of x^n corresponding to the number of planted plane trees with n edges.

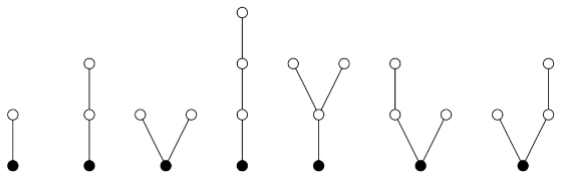

Figure 9: The possible non-isomorphic planted plane trees with 1, 2, 3 and 4 edges respectively.

In conclusion, from setting up and manipulating the *generating function* for a previously unknown sequence of numbers, we have extracted what these numbers actually are. Generating functions of a certain class of objects (labelled trees, decorated trees, etc.) will prove very useful not only in enumeration - as I have attempted to briefly show here - but even more so in deriving recursive relations for these functions from intrinsic properties of the class of trees that one is interested in. From there, we will see how this can help us to obtain information on the distance statistics within these trees.

3 Regular Quadrangulations

This section is about *regular* (i.e. unicolored) quadrangulations of the plane, and more importantly their bijection with a specific class of plane trees. In contrast to the following section on *Eulerian* quadrangulations, this is quite a well-studied topic - at least within the context of two-dimensional quantum gravity.

Figure 10: A quadrangulation of the plane.

To start off, I would like to give some motivation as to why we would be looking for a bijection between these two objects in the first place. To illustrate this, the following two results by one of the pioneers of the study of maps, W.T. Tutte (1917- 2002), are of great use.

Theorem 3.1. ***Tutte's Bijection.*** *For any g and n there is an explicit bijection between rooted maps of genus g with n edges and rooted quadrangulations of genus g with n faces.*

Not only in our case will this be a useful theorem - it uniquely translates any map with arbitrary face degrees into a quadrangulation (i.e. with *bounded* face degrees), which is generally far easier to work with.

Theorem 3.2. *The number of rooted planar maps with n edges, is*

$$\frac{2 \cdot 3^n}{n+2} C_n \tag{15}$$

with C_n as in the previous section.

Interesting notes and even thorough proofs of these two theorems can be found in [7]. Surprisingly, we see the Catalan number C_n popping up in the enumeration of planar maps, and thus - via Tutte's bijection - in that of planar quadrangulations as well. Hence, it seems quite natural to look for a bijection between quadrangulations and plane trees, possibly decorated with some additional information.

3.1 The Schaeffer Bijection

Firstly, let us define the 'class of trees' that we are looking for.

Definition 3.3. A *well-labelled tree* is a tree in which every vertex has a label $n \in \mathbb{N}_{>0}$, obeying:

- the labels vary by *at most* one between neighbours;
- the minimal label on the tree is 1.

Now we are ready to state what is probably the most important result of this section.

Theorem 3.4. ***Schaeffer's Bijection****. There exists a bijection between rooted and pointed quadrangulations with n faces and rooted well-labeled trees with n edges.*

Pointing the quadrangulation means marking one specific vertex as the 'origin'. Rooting the quadrangulation in this case corresponds to marking and edge between two vertices with labels $(l-1)$ and l with an orientation $(l-1) \to l$.
The marked vertex will become the starting point of the construction of the corresponding well-labelled tree.
As an extension of (3.1) and (3.2), an exact enumerative proof that the set $|W_n|$ of rooted well-labelled with n edges is precisely equal to $|Q_n|$ of rooted and pointed quadrangulations with n faces can be found in [8]. Let us now turn to the construction of the bijection.

3.1.1 Construction: From Quadrangulation to Tree

Our goal is to obtain a mapping $\Psi : \mathcal{Q} \to \mathcal{T}$ that constructs a rooted well-labelled tree $T \in \mathcal{T}$ out of a rooted and pointed quadrangulation $Q \in \mathcal{Q}$. I will visually try to explain *step-by-step* what the construction looks like.

1. We start with a rooted and pointed planar quadrangulation Q.

2. We label the pointed vertex with label 0 and subsequently label every vertex of Q with its *geodesic distance* from the pointed vertex, i.e. the length of the shortest path from the considered vertex to the pointed vertex.

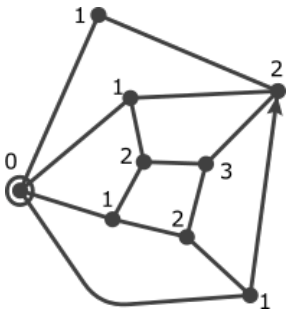

3. Next, we observe that we have in general two types of faces within the labelled quadrangulation. We apply the rules of figure 11 to draw an edge within every face of Q.

4. After drawing the new edges and erasing the old edges of Q along with the pointed vertex, we are left with figure 12. The vertex of Q that the root edge points

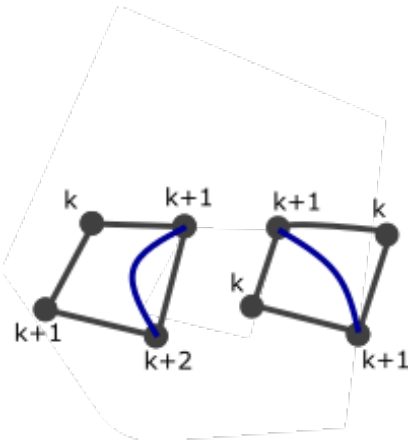

Figure 11: The local rules.

towards, now becomes the root of the well-labelled tree T. To recover the root edge in the inverse process, instead of indicating the root of a tree with an arrow we now indicate it by marking a specific *corner* belonging to the root vertex.

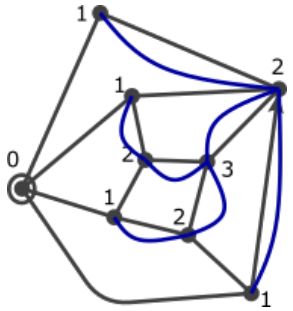

For a thorough proof that the resulting graph is indeed a well-labelled tree, I would like to refer the reader to [10] or alternatively [8]. It follows that $T \in \mathcal{T}$. $\square$

3.1.2 Construction: From Tree to Quadrangulation

The inverse $\Phi : \mathcal{T} \to \mathcal{Q}$ of the construction above is a tad more difficult, but naturally I will try to give an as clear as possible explanation of the construction of a rooted and pointed quadrangulation $Q \in \mathcal{Q}$ out of a rooted well-labelled tree $T \in \mathcal{T}$.

1. This time we start with a rooted well-labelled tree T; let us for the sake of simplicity take the tree of figure 12.

2. We insert a *leg* in every corner of T.

3. Starting from the root vertex, we connect every leg belonging to a vertex of label $i > 1$ to the first vertex of label $i - 1$ we encounter while walking around T in *counter-clockwise* order. These new edges become the edges of Q. The edge that is drawn out of the *root corner* of T in this process, becomes the root edge of Q with an orientation $(l - 1) \to l$ as before. Rather surprisingly, this 'matching process' is unique up to homeomorphisms.

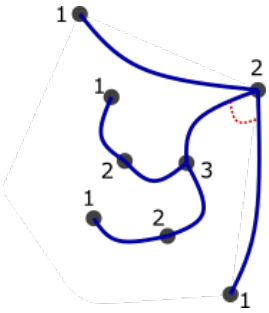

Figure 12: The resulting well-labelled tree. The root corner is indicated by the dashed red line.

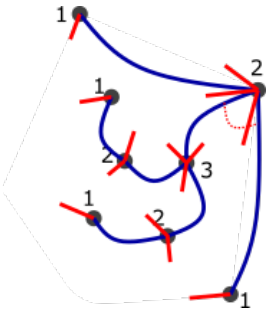

4. Next, we place a vertex with label 0 in the only face of T and connect every leg belonging to a vertex with label 1 to this vertex. The vertex with label 0 becomes the pointed vertex of the quadrangulation.

5. After drawing the new edges of Q and erasing the original edges of T, we have recovered a rooted and pointed quadrangulation out of a rooted well-labelled tree. Note that the edge that had the root corner as its starting point has become the root edge.

The proof that the resulting graph must be a quadrangulation and - more importantly - that $\Phi = \Psi^{-1}$ is indeed the *inverse* of the construction from section 3.1.1, is rather technical and slightly outside the scope of this thesis. I would rather like to refer any interested reader to [8] if they wish to know more.
We have now successfully constructed Schaeffer's bijection between the set $\mathcal{Q}$ of pointed and rooted quadrangulations and the set $\mathcal{T}$ of rooted well-labelled trees. Let us also define the following two properties of quadrangulations and trees respectively [8].

Definition 3.5. The *label distribution* of a well-labelled tree T is the sequence $(\lambda_k^T)_{k>0}$ of the number of vertices of T with label k.
The profile of a planar quadrangulation Q is the sequence $(\pi_k^Q)_{k>0}$ of the number of vertices of Q at geodesic distance k from the pointed vertex.

Please note the following interesting feature of the Schaeffer bijection.

Remark. The Schaeffer bijection works exactly in such a way, that $\Psi : \mathcal{Q} \to \mathcal{T}$ maps the *profile* $(\pi_k^Q)_{k>0}$ of Q onto the *label distribution* $(\lambda_k^T)_{k>0}$ of T and, vice versa for the inverse Φ.

This will give us a surprisingly natural way to consider distances within any quadrangulation by looking at the labels on the corresponding trees.

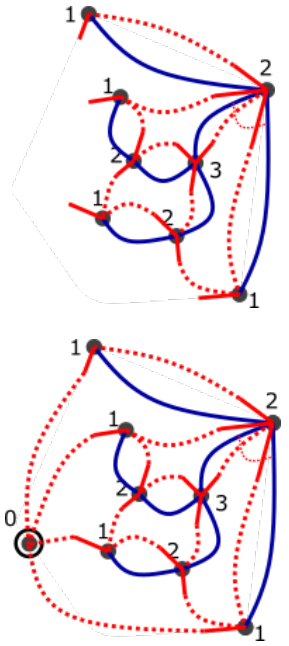

3.2 Distances in Random Quadrangulations: From The Labelling Of The Trees

At the start of this section on distances within random quadrangulations, it might be useful to state what we are actually interested in. Since we are dealing with pointed *and* rooted quadrangulations, naturally two of the vertices are marked *at random*. We wish to be able to say something about the *distribution* of the distance between these two vertices in large quadrangulations. This, however, turns out to be quite a challenge. Before diving into that, I would like to give a more insightful explanation as to why these distances of order $n^{1/4}$ are actually quite intuitive, only using the labels of the corresponding trees. To that end, suppose we select a third vertex in the quadrangulation uniformly at random, and look at the label of this vertex. Let us denote the label of the root vertex by d_1, and the label of this new vertex by d_2. In the previous section, we have discovered that the distribution of the labels on the well-labelled tree corresponding to a quadrangulation of the plane is one-to-one with the distribution of the geodesic distance of the vertices of the quadrangulation from the pointed vertex with label 0. Now, we can not yet say anything constructive about the distribution of the distances d_1 and d_2 themselves, but we might be able to say something about the distribution of the *difference* between the geodesic distances d_1 and d_2, $D \equiv d_2 - d_1$, and how this difference depends on the number of squares n. From Schaeffer's bijection, we will straightforwardly be able to convert this to *the difference of the labels* on the path from the root of the tree, labelled d_1, to the selected vertex labelled d_2.
In a natural way, we can now divide the problem into two parts - one that takes into account the distribution of the labels on the tree when we take a walk from the root of the tree to a randomly chosen vertex in the tree at distance r; and one that calculates this distribution of this 'height' r of a randomly chosen vertex within the tree as a function of the total number of edges, n.

Figure 13: After completing step 5, we recovered the quadrangulation from figure 1.

3.2.1 The distribution of the labels

Recall the definition of a well-labelled tree 3.3, where the vertices of the tree are labelled with a number that can only change by $0, \pm 1$ going from one vertex to another. Therefore, let us quickly note the following:

Remark. Alternatively, we can label every edge of the tree by their *increment* as we walk away from the root of the tree.

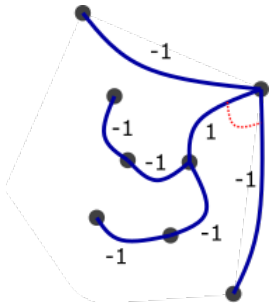

Figure 14: The tree of figure 12 with the edges labelled instead of the vertices.

Even though figure 14 might suggest otherwise, naturally the labelling that we obtain in this way is uniformly distributed among all possible labels in $\{-1, 0, 1\}^n$, and we might suggestively write that the labelling of a well-labelled tree of n edges is of the form *tree* $+ \{-1, 0, 1\}^n$. We can subsequently write the sum of the labels D as

$$D = \sum_{i=1}^{r} \varepsilon_i, \tag{16}$$

where the ε_i are independent random variables chosen uniformly in $\{-1, 0, 1\}$. Since this labelling distribution is symmetric around zero, we expect $\langle D \rangle = 0$. Therefore, we need to find another way to gain information on D. It is natural to look at the variance

$\langle D^2 \rangle$. Since all of the 'steps' are independent, this is simply computed to be

$$\begin{aligned}\langle D^2 \rangle &= \left\langle \left(\sum_{i=1}^{r} \varepsilon_i \right)^2 \right\rangle \\ &= \left\langle \sum_{i=1}^{r} \sum_{j=1}^{r} \varepsilon_i \varepsilon_j \right\rangle \\ &= \left\langle \sum_{i=1}^{r} \varepsilon_i^2 \right\rangle \\ &= r \cdot \langle \varepsilon_1^2 \rangle = \frac{2}{3} n,\end{aligned}$$

and finally we find

$$\langle D^2 \rangle \propto r, \tag{17}$$

which is - because of the fact that $\langle D \rangle = 0$ - an explicit relation between the variance of D and the height r of a randomly chosen vertex on the tree.

3.2.2 The height of a randomly chosen vertex of a tree

The next part of our quest is to determine how the height of a randomly chosen vertex in a tree, r, depends on the number of edges n of the tree, in the large n limit. To this end, let us define the following.

Definition 3.6. A *Dyck path* is a walk from $(0, 0)$ to $(2n, 0)$ in the plane, without ever going below the x-axis.

One can also characterize the contour walk along the edges of a tree by a *Dyck path*. Intuitively, this is in correspondence with plane trees, as well as the regular bracket structures from the previous section.

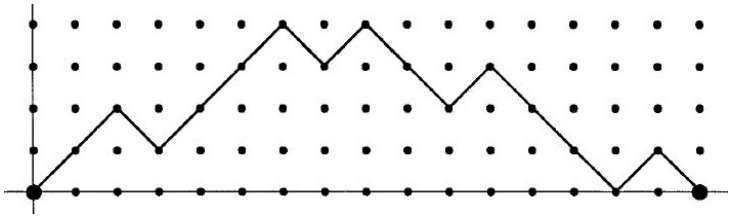

Figure 15: One of the possible Dyck paths for $n = 8$. Image credit: slideplayer.com.

Observing that the figures 15 and 16 are in bijection with each other, is completely identical to the procedure for the regular bracket structures. Starting from the root of the plane tree and taking a walk in clockwise direction around the edges of the tree, we associate a step upwards in the Dyck path with a step moving away from the root of the tree, and vice versa. The walk will traverse each edge twice, once upwards and once downwards.
The following theorem will be of great use to us. [6]

Theorem 3.7. *The sum of the areas of all Dyck paths $\mathcal{D}_{2n}$ of length $2n$ is given by*

$$\sum_{P \in \mathcal{D}_{2n}} Area(P) = 4^n - \frac{1}{2} \binom{2n+2}{n+1}. \tag{18}$$

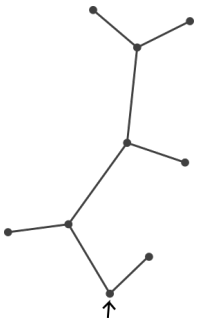

Figure 16: The plane tree corresponding to the Dyck path of figure 15.

Naturally, the average height r is now equal to this sum divided by the length per path and the total number of Dyck paths of length $2n$.
Let us now calculate this average height r in a tree with n edges.

$$\begin{aligned}\langle r\rangle &= \frac{\text{total area}}{\text{length per path} \times \text{number of paths}} \\ &= \frac{4^n - \frac{1}{2}\binom{2n+2}{n+1}}{2n \cdot C_n} \\ &= \frac{4^n}{2n \cdot C_n} - \frac{\frac{1}{2}\binom{2n+2}{n+1}}{2n \cdot C_n}.\end{aligned}$$

Before we move on, we have to note that the right side of the last expression looks a lot like something that might become constant in the large n limit. Let us explicitly calculate that this is indeed the case. By definition of the Catalan number,

$$\frac{\binom{2n+2}{n+1}}{4n \cdot C_n} = \frac{\binom{2n+2}{n+1}}{\binom{2n}{n}} \frac{n+1}{4n}.$$

Now we note that $\binom{2n+2}{n+1} = \binom{2n}{n} \frac{(2n+2)(2n+1)}{(n+1)(n+1)}$, and therefore

$$\begin{aligned}&\frac{\binom{2n+2}{n+1}}{\binom{2n}{n}} \frac{n+1}{4n} \\ &= \frac{(2n+2)(2n+1)}{4n(n+1)}.\end{aligned}$$

Taking the limit of $n \to \infty$, we find that

$$\frac{(2n+2)(2n+1)}{4n(n+1)} = \frac{4n^2}{4n^2} = 1, \tag{19}$$

and we conclude that $\binom{2n+2}{n+1} \sim 4n \cdot C_n$ in the limit of large n. [2]
We may forget this term for now, since it does not explicitly depend on n. Let us

[2] $f(n) \sim g(n)$ is defined as $\lim_{n\to\infty} f(n)/g(n) = 1$.

continue, and write

$$\begin{aligned}\langle r\rangle &\sim \frac{4^n}{2n\cdot C_n}\\ &= \frac{4^n}{2n}\frac{(n+1)\cdot(n!)^2}{(2n)!}\\ &\sim \frac{4^n}{2}\frac{2\pi n\left(\frac{n}{e}\right)^{2n}}{\sqrt{4\pi n}\left(\frac{2n}{e}\right)^{2n}}\\ &= \frac{4^n}{2}\cdot\left(\frac{1}{2}\right)^{2n}\frac{2\pi n}{\sqrt{4\pi n}},\end{aligned}$$

where we used *Stirling's approximation* for factorials of large numbers:

$$n!\sim\sqrt{2\pi n}\left(\frac{n}{e}\right)^n.$$

In the end, we find the surprisingly simple formula

$$\langle r\rangle \sim \frac{1}{2}\sqrt{\pi n}, \tag{20}$$

and hence, we have found the dependence $\langle r\rangle \propto \sqrt{n}$ for the height of a randomly chosen vertex in the tree on the number of edges n. Combined with the previous section, this means that we have established the variance of our distance D to scale with the square root of n and, hence, its standard deviation to scale with $n^{\frac{1}{4}}$. This means that upon choosing 3 different points on the quadrangulation and observing the distance between one select point and the other two, the difference between these two distances will generally be of order $n^{\frac{1}{4}}$. This does not yet prove that d_1 or d_2 themselves are typically of order $n^{\frac{1}{4}}$. If we quickly make the assumption that d_1 and d_2 are equally distributed, we might try to compute a lower bound on $\langle d_1^2\rangle$, by

$$\langle D^2\rangle = \langle (d_2-d_1)^2\rangle = \langle d_1^2+d_2^2-2d_1d_2\rangle \leq \langle 2d_1^2\rangle \Rightarrow \langle d_1^2\rangle \geq \frac{1}{2}\langle D^2\rangle \tag{21}$$

and find that a lower bound is given by $\langle D^2\rangle/2$. This means that the standard deviation on d_1 is minimally given by something that is of order $n^{\frac{1}{4}}$. This is already a clear indication that, as n grows large, distances between two randomly selected points will perhaps be of order $n^{\frac{1}{4}}$ themselves.

3.3 Distances in Random Quadrangulations: The Two Point Function

As a more rigorous and slightly more exact approach, we can try to tackle the problem using the framework of generating functions (see 2.2). This is where we really start to appreciate working with generating functions.
In our bijection, introduced in section 3.1, we found that a pointed quadrangulation with a marked oriented edge pointed towards a vertex at geodesic distance k is in one-to-one correspondence with a well-labelled tree with root label k. In this section we wish to establish a generating function for well-labelled trees *that keeps track of the root label*. This means that we will index our generating function with parameter that will indicate the root label of the considered trees. This concept of constructing a generating function that keeps track of distances - in our case, the distance between the pointed vertex and the root edge of the quadrangulation - is more commonly known as the *two-point function*.

Let us denote the generating function of planar quadrangulations with the end of the root edge at geodesic distance k by $G_k(x)$, and quickly remind ourselves that the corresponding well-labelled tree has root label k. The expansion of the generating function $G_k(x)$ is then given by

$$G_k(x) = \sum_{n=0}^{\infty} G_{k,n} x^n, \tag{22}$$

where the coefficient of x^n denotes the number of vertices at geodesic distance k from the pointed vertex in a quadrangulation with n squares.
To make our life easier, let us quickly define the following:

Definition 3.8. An *almost well-labelled tree* is a well-labelled tree on which the restriction that the minimal label must be 1 is lifted. All the labels must still be positive, and the labels on the vertices can still only differ by $0, \pm 1$ along the edges.

Firstly, we wish to determine a generating function of almost well-labelled trees with root label equal to this value, k. In this case, almost well-labelled trees are easier to work with than well-labelled trees, because other than positivity, there are no restrictions on the actual values of their labels; only on the value of the difference of two consecutive labels. Let us denote their generating function by $R_k(x)$. Since $R_k(x)$ generates almost well-labelled trees with root label k, we need to take into account only those elements of R_k that have a minimal label 1 somewhere on the tree to recover $G_k(x)$ from $R_k(x)$. This is achieved by a simple shift of labels from $k \to k-1$ and then subtracting - i.e.

$$G_k = R_k - R_{k-1}. \tag{23}$$

Because the elements of G_k are in bijection with pointed and rooted quadrangulations of the plane with two marked points at geodesic distance k, this mechanism of shifting the labels shows us that the elements of R_k are in bijection with rooted and pointed quadrangulations with *two marked points at geodesic distance* $\leq k$. The amount by which we have to shift down the labels to obtain a well-labelled tree out of an almost well-labelled tree, is determined by the minimal label of said well-labelled tree. Subsequently, let us try to explicitly calculate this generating function $R_k(x)$.

3.3.1 The Generating Function of Almost Well-Labelled Trees

Suppose we have a function $R_k(x)$, generating an almost well-labelled tree with root label k. Let us now consider *all* the different possibilities for the tree to branch outwards from the root. In theory, we might have $n \in \mathbb{N}$ new branches into new vertices of the tree, all connected by edges with equal weight x and these new branches have three possible labels from the label restriction on almost well-labelled trees - namely, $k-1, k$ or $k+1$. Each of these branches corresponds to the root of a new tree, starting at that vertex, and hence they are enumerated by $R_{k-1}(x), R_k(x)$ and $R_{k+1}(x)$ respectively.

This implies the relation

$$R_k(x) = \sum_{n=0}^{\infty} x^n \left(R_{k-1}(x) + R_k(x) + R_{k+1}(x)\right)^n, \tag{24}$$

and we obtain the recurrence relation

$$R_k(x) = \frac{1}{1 - x\left(R_{k-1}(x) + R_k(x) + R_{k+1}(x)\right)}, \tag{25}$$

or equivalently,

$$R_k(x) = 1 + xR_k(x)\left(R_{k-1}(x) + R_k(x) + R_{k+1}(x)\right). \tag{26}$$

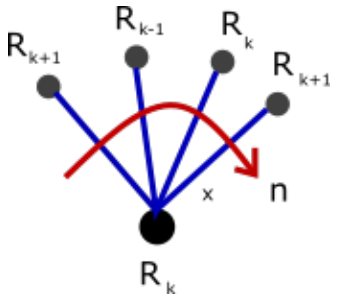

Figure 17: Some of the possibilities for a tree, with generating function R_k, to branch into new trees.

Generally, this is far from easy to solve, because the equation at hand is recursive and more importantly non-linear. However, we might be able to make an attempt at linearizing the equation. The recursive equation that we will obtain in the next section on Eulerian Quadrangulations will be even more troublesome to solve analytically, and there we will need to resort to a so called *continuum limit* approach. I will also introduce this in the next section to solve the problem at hand, but at first we are quickly going to investigate how to solve (26) more exactly following the lines of [2].

3.3.2 Exact Solution to the Recurrence Relation

Firstly, I want to point out that we need to impose two conditions. For a start, we need to have an initial condition $R_0 = 0$; and secondly we need to have that in the large k limit, we obtain

$$\lim_{k\to\infty} R_k = R_\infty \tag{27}$$

$$= \frac{1-\sqrt{1-12x}}{6x}, \tag{28}$$

where R_∞ is the solution to the quadratic equation

$$R_\infty = 1 + 3xR_\infty^2, \tag{29}$$

as can be established by letting k go to infinity in equation (26). The solution R_∞ displays the 'critical value' of $x_c = \frac{1}{12}$ of pure quadrangulations. This value of x_c precisely corresponds to the radius of convergence of the generating function R_∞. More on this critical value will follow in section 3.3.3.
Let us now expand R_k in the vicinity of R_∞, and write

$$R_k = R_\infty(1-\rho_k). \tag{30}$$

Upon substituting this in (26) and only keeping the terms that are linear in ρ, we obtain the following equation, which can be seen as the 'first order linearization' of (26),

$$-R_\infty\rho_k^{(1)} = -3xR_\infty^2\rho_k^{(1)} - xR_\infty^2\left(\rho_{k-1}^{(1)} + \rho_k^{(1)} + \rho_{k-1}^{(1)}\right)$$

or equivalently,

$$\rho_k^{(1)} = 3xR_\infty\rho_k^{(1)} + xR_\infty\left(\rho_{k-1}^{(1)} + \rho_k^{(1)} + \rho_{k-1}^{(1)}\right). \tag{31}$$

By setting $\rho_k^{(1)} = \alpha_1\, y^k$, we obtain the *characteristic equation* for this recurrence relation, given by

$$y^k = xR_\infty \left(y^{k-1} + y^k + y^{k+1}\right) + 3xR_\infty y^k \Longrightarrow \frac{1-4xR_\infty}{xR_\infty} = \frac{1}{y} + y. \tag{32}$$

Here it is important that we impose the condition $|y| < 1$, to ensure $\lim_{k\to\infty} \rho_k^{(1)} = 0$ and hence the convergence of R_k to R_∞. We can now expand R_k further in ρ_k, by writing ρ_k fully as a power series of the solution to the characteristic equation y^k, by writing

$$\rho_k = \sum_{i=1}^{\infty} \alpha_i (y^k)^i. \tag{33}$$

Substituting this into equation (30), then substituting equation (26) for R_k and finally picking the terms of order $l+1$ in y^k, and remembering that if two power series coincide, the coefficients of their powers must coincide, we obtain a relation for the coefficients of α_k of equation (33):

$$\alpha_{l+1}\left(y^{l+1} + \frac{1}{y^{l+1}} - y - \frac{1}{y}\right) = \sum_{j=1}^{l} \alpha_j \alpha_{l+1-j}\left(y^j + \frac{1}{y^j} + 1\right). \tag{34}$$

The reader might check by themselves that this relation holds. The products $\alpha_j\alpha_{l+1-j}$ originate from the products $R_k\left(R_{k+1} + ...\right)$ in equation (26) - where j sums over all the possibilities to obtain a power of $l+1$ in y^k out of the two terms.
Now that we have obtained a recursive relation for the coefficients of the power series ρ_k, it is possible to give a closed form solution for R_k in terms of R_∞ and the solution to the characteristic equation y. For the purpose of this thesis I do not think it is necessary to repeat all the steps, but an interested reader may find the derivation in [2].
The final solution to the recurrence relation (26) becomes

$$R_k = R_\infty \frac{(1-\lambda y^{k+1})(1-\lambda y^{k+4})}{(1-\lambda y^{k+2})(1-\lambda y^{k+3})},$$

where λ is an arbitrary constant. Upon imposing our initial condition $R_0 = 0$, we find that the only λ that will ensure $R_0 = 0$ *and* ensure the convergence of R_k to R_∞ in the limit $k \to \infty$, will be $\lambda = y^{-1}$. Substituting this into our last result, we obtain

$$R_k = R_\infty \frac{(1-y^k)(1-y^{k+3})}{(1-y^{k+1})(1-y^{k+2})}. \tag{35}$$

It may be explicitly checked that this final solution precisely solves our recurrence relation (26).

3.3.3 Critical Scaling

Now that we have found an exact solution, we might be interested to see how this solution behaves in the limit where the number of squares of the quadrangulation, n, becomes large. As mentioned before, the critical value x_c corresponds to the radius of convergence of the generating function R_∞, the generating function for planar quadrangulations without restrictions on distances between two marked points. As a continuum limit, we might study this generating function as x tends to its critical value of $x_c = \frac{1}{12}$ (see equation 27). To that end, let us set

$$x = x_c(1-\Lambda\epsilon^4) = \frac{1}{12}(1-\Lambda\epsilon^4). \tag{36}$$

The quantity Λ should be interpreted as a cosmological constant, and is related to the total volume V of the map by an explicit Laplace transform. This Laplace transform can be viewed as the *continuum limit* of the generating function for planar quadrangulations. To make this more clear, let us say that planar quadrangulations with n squares, without restrictions on the distance between two points, are enumerated by Q_n. As we know, we can denote its generating function as

$$R_\infty(x) = \sum_n Q_n \, x^n. \tag{37}$$

Let us quickly state the following, very useful, theorem [11]:

Theorem 3.9. ***Transfer Theorem for singularity analysis.*** *Let $A(z)$ be a generating function with its closest singularity at $z = \rho$, and there it has an expansion of the form*

$$A(z) = a_0 + a_1 \, (1 - z/\rho)^{-\alpha} + \mathcal{O}\left((1 - z/\rho)^{-\alpha+1}\right), \tag{38}$$

then, in the limit of large n, its coefficients grow as:

$$[z^n]A(z) \sim c \; n^{\alpha-1}\rho^{-n} \tag{39}$$

We can immediately apply this theorem to our form of the function R_∞ from equation (27). We have a singularity of the form $(1-x/x_c)^{1/2}$, so in this case the leading order of our expansion has $\alpha = -1/2$. Applying the theorem, we readily see that the coefficients of R_∞ behave asymptotically as

$$Q_n \sim C \; x_c^{-n} \; n^{-3/2}, \tag{40}$$

for some constant C. Now, we may use the expansion of equation (36) to write

$$R_\infty(x) = C \; \sum_n x_c^{-n} \; n^{-3/2} \left(x_c \, (1 - \Lambda\epsilon^4)\right)^n. \tag{41}$$

Since we have chosen a scaling of $(x_c - x) \propto \epsilon^4$ for the edges of our trees - and hence the faces of the quadrangulations, we may write that the total volume of the map in this case is related to the total number of squares n by

$$V = n\epsilon^4. \tag{42}$$

We can subsequently change the sum over n into an integral over the *continuum volume* V, in the limit $\epsilon \to 0$, as

$$\lim_{\epsilon\to 0} R_\infty(x) = C \int_0^\infty \frac{dV}{\epsilon^4} \; x_c^{-n} \left(\frac{V}{\epsilon^4}\right)^{-3/2} x_c^n \left(1 - \Lambda\epsilon^4\right)^{\frac{V}{\epsilon^4}} \tag{43}$$

$$\approx C \int_0^\infty \frac{dV}{\epsilon^4} \; \left(\frac{V}{\epsilon^4}\right)^{-3/2} \; e^{-\Lambda V} \tag{44}$$

$$\equiv \; C\epsilon^2 \int_0^\infty dV \; \mathcal{R}_V \; e^{-\Lambda V} \equiv \; C\epsilon^2 \; \mathcal{R}_\Lambda. \tag{45}$$

One thing that has to be noted here, is that this is in essence a 'formal' integral: for our value of $-3/2$ as the power of V, it does not converge at $V = 0$. From this, it is readily seen that in the limit of large n the integral is strongly dominated by quadrangulations of small volume. This is also seen by the fact that in this limit, R_∞ obtains just a *tiny* contribution from these large quadrangulations, of order ϵ^2 (as seen in the last line of the previous equation). We will shortly see how to resolve this problem, and

more importantly how this Laplace transformation might be able to help us to obtain information on the scaling limit of large quadrangulations. Firstly, let us quickly return to the exact solution to the recursion relation (26). From a clever inspection of equation (27), we see that our expansion of equation (36) corresponds to

$$6xR_\infty = 1 - \sqrt{\Lambda\epsilon^4} \rightarrow xR_\infty = \frac{1}{6}(1 - \Lambda^{1/2}\epsilon^2). \tag{46}$$

Then, from the characteristic equation (32), we find that y can be written as

$$\frac{1 - 4xR_\infty}{xR_\infty} = 2 + a^2\epsilon^2 + \mathcal{O}(\epsilon^3) = e^{a\epsilon} + e^{-a\epsilon} + \mathcal{O}(\epsilon^3) \rightarrow y = e^{\pm a\epsilon} + \mathcal{O}(\epsilon^3), \tag{47}$$

where a can be determined from combining equation (46) and (47) by writing

$$6 - 4(1 - \Lambda^{1/2}\epsilon^2) = (y + \frac{1}{y})(1 - \Lambda^{1/2}\epsilon^2),$$

and filling in the series expansion for $y = e^{-a\epsilon}$ and subsequently collecting all powers of ϵ^2 to obtain $a = \sqrt{6\Lambda^{1/2}}$.
Filling in this ansatz for y in the exact solution to our recurrence relation, we find that

$$R_k = R_\infty \frac{\left(1 - (e^{-a\epsilon})^k\right)\left(1 - (e^{-a\epsilon})^{k+3}\right)}{\left(1 - (e^{-a\epsilon})^{k+1}\right)\left(1 - (e^{-a\epsilon})^{k+2}\right)}. \tag{48}$$

Subsequently, since we want to investigate the limit where ϵ goes to zero and distances between points grow large, we rewrite the geodesic distance k in terms of a *continuum scaling variable* r as

$$k = \frac{r}{\epsilon^\alpha},$$

and letting ϵ go to zero. If we now wish to determine the power a of ϵ, let us expand all the exponentials in equation (48) up to second order as

$$R_k = R_\infty \frac{(a\epsilon k - \frac{1}{2}a^2\epsilon^2k^2)\,(1 - \,(1 - a\epsilon k + \frac{1}{2}a^2\epsilon^2k^2)\,(1 - 3a\epsilon + \frac{1}{2}9a^2\epsilon^2))}{(1 - \,(1 - a\epsilon k + \frac{1}{2}a^2\epsilon^2k^2)\,(1 - a\epsilon + \frac{1}{2}a^2\epsilon^2))(1 - \,(1 - a\epsilon k + \frac{1}{2}a^2\epsilon^2k^2)\,(1 - 2a\epsilon + \frac{1}{2}4a^2\epsilon^2))},$$

from which it is quite straightforwardly observed that a sensible continuum limit is obtained in the case where $k \propto \epsilon^{-1}$ as ϵ goes to zero, to ensure that neither the numerator nor the denominator does evaluate to zero in this limit, and furthermore that we have $\lim_{\epsilon\to 0} R_k = R_\infty$. Finally, we find

$$k = \frac{r}{\epsilon} \tag{49}$$

for the scaling between k and ϵ. From this we can actually already draw the small conclusion that, apparently, there is a relation between the ϵ-scaling that we *choose* for the faces of the map in the limit $x \rightarrow x_c$, and the scaling that follows for the geodesic distance k, and it just so appears to have a fourth power between them.
This continuum scaling variable r that has been defined by equation (49) is precisely the variable that keeps track of geodesic distances within the continuum volume V of our map, as defined by equation (42). To make this more precise, we might write (recall equation (22)!)

$$\lim_{\epsilon\to 0} \frac{1}{\epsilon^3 R_\infty} G_k(x) = \lim_{\epsilon\to 0} \frac{1}{\epsilon^3 R_\infty} \sum_{n=0}^{\infty} G_{k,n}\, x^n = \mathcal{G}_\Lambda(r) = \int_0^\infty dV\; \mathcal{G}_V(r)\, e^{-\Lambda V}, \tag{50}$$

where in this case in our continuum space, $G_\Lambda(r)$ is the *continuum partition function* for surfaces with two marked points at geodesic distance r within volume V.

We can now calculate explicitly what this function $G_\Lambda(r)$ should be. To that end, let us recall that the exact solution to the recursion relation (26), $R_k(x)$, generates planar quadrangulations with two marked points at geodesic distance $\leq k$. However, in our formulation of the Laplace transform of (43) we encountered the problem that in the continuum limit, R_k will always be dominated by quadrangulations of very small sizes n and small geodesic distances k. This is not what we are looking for, because we are interested in the scaling of geodesic distances in the case where the sizes of quadrangulations are very large. Therefore, it is much more useful to look at the generating function $R_\infty - R_k$ of quadrangulations with two marked points at a *geodesic distance* $\geq k$. This immediately resolves the issue of the Laplace transform, in the limit of large quadrangulation sizes and large geodesic distances!
Similar to the function $G_\Lambda(r)$ as defined by (50), we can now define the continuum partition function for surfaces with two marked points at geodesic distance $\geq k$ (in which, for now, I will be omitting the subscript Λ) as

$$\mathcal{F}(r) \equiv \lim_{\epsilon \to 0} \frac{R_\infty - R_k}{\epsilon^2 R_\infty}, \tag{51}$$

in which we have divided by R_∞ by means of convention. Let us quickly rewrite this as

$$R_k = R_\infty \left(1 - \epsilon^2 \mathcal{F}(k\epsilon)\right). \tag{52}$$

One may notice that this does actually look a lot like the expansion that was made in (30)! Equation (52) can be seen as the 'continuum' equivalent of (30).
We see that we have an expression for R_k in terms of the function $\mathcal{F}$, which is yet to be determined. To determine this function, let us plug (52) into (26). We obtain

$$R_\infty \left(1 - \epsilon^2 \mathcal{F}(k\epsilon)\right) = 1 + xR_\infty^2 (1 - \epsilon^2 \mathcal{F}(k\epsilon)) \left((1 - \epsilon^2 \mathcal{F}(k\epsilon + \epsilon)) + (1 - \epsilon^2 \mathcal{F}(k\epsilon)) + (1 - \epsilon^2 \mathcal{F}(k\epsilon - \epsilon))\right). \tag{53}$$

Now, we will expand this equation up to fourth order in ϵ. To make this procedure a bit more comprehensible, let us first organize the different terms according to their order. We look at equation (53) and gather all the different orders together up to order 4, as they appear in equation (53).

$$\mathcal{O}(1) : R_\infty = 1 + 3xR_\infty^2$$
$$\mathcal{O}(\epsilon^2) : -\epsilon^2 R_\infty \mathcal{F}(r) = -3xR_\infty^2 \epsilon^2 \mathcal{F}(r) - xR_\infty^2 \epsilon^2 \left(\mathcal{F}(r+\epsilon) + \mathcal{F}(r) + \mathcal{F}(r-\epsilon)\right)$$
$$\mathcal{O}(\epsilon^4) : 0 = xR_\infty^2 \epsilon^4 \mathcal{F}(r) \left(\mathcal{F}(r+\epsilon) + \mathcal{F}(r) + \mathcal{F}(r-\epsilon)\right).$$

Our first observation, is that the terms of order one precisely correspond to (27), as should be the case. They cancel each other. Subsequently, we divide everything by R_∞ and substitute the expression from equation (46) for xR_∞, and we obtain

$$\mathcal{O}(\epsilon^2) : -\epsilon^2 \mathcal{F}(r) = -\frac{3}{6}(1 - \Lambda\epsilon^2)\epsilon^2 \mathcal{F}(r) - \frac{1}{6}(1 - \Lambda\epsilon^2)\epsilon^2 \left(\mathcal{F}(r+\epsilon) + \mathcal{F}(r) + \mathcal{F}(r-\epsilon)\right)$$
$$\mathcal{O}(\epsilon^4) : 0 = \frac{1}{6}(1 - \Lambda\epsilon^2)\epsilon^4 \mathcal{F}(r) \left(\mathcal{F}(r+\epsilon) + \mathcal{F}(r) + \mathcal{F}(r-\epsilon)\right).$$

Let us do the exact same thing again: we distinguish the terms of order ϵ^2 and those of order ϵ^4. However, we now remember that they were all part of the same equation (53), and therefore the equations corresponding to the different orders ultimately should be added up. Upon doing this, and immediately taking the ϵ^2-terms to the left side of the equation and the ϵ^4-terms to the right side, this yields

$$-\frac{3}{6}\epsilon^2 \mathcal{F}(r) + \frac{1}{6}\epsilon^2 \left(\mathcal{F}(r+\epsilon) + \mathcal{F}(r) + \mathcal{F}(r-\epsilon)\right) = \frac{3}{6}\Lambda^{1/2}\epsilon^4 \mathcal{F}(r) +$$
$$\frac{1}{6}\Lambda^{1/2}\epsilon^4 \left(\mathcal{F}(r+\epsilon) + \mathcal{F}(r) + \mathcal{F}(r-\epsilon)\right) + \frac{1}{6}\epsilon^4 \mathcal{F}(r) \left(\mathcal{F}(r+\epsilon) + \mathcal{F}(r) + \mathcal{F}(r-\epsilon)\right) + \mathcal{O}(\epsilon^6).$$

Organizing, dividing by ϵ^4, multiplying by a factor of 6 and finally taking the limit $\epsilon \to 0$, as in our definition of the function $\mathcal{F}(r)$ (51), we see that this corresponds to

$$\lim_{\epsilon\to 0} \frac{1}{\epsilon^2} \left(\mathcal{F}(r+\epsilon) + 2\mathcal{F}(r) + \mathcal{F}(r-\epsilon)\right) = 6\Lambda^{1/2}\mathcal{F}(r) + 3\mathcal{F}^2(r) + \mathcal{O}(\epsilon^2),$$

or equivalently, using the definition of the second derivative of a function, we obtain the following second order differential equation for $\mathcal{F}(r)$:

$$\frac{d^2\mathcal{F}(r)}{dr^2} - 6\Lambda^{1/2}\mathcal{F}(r) - 3\mathcal{F}^2(r) = 0 \tag{54}$$

This differential equation was obtained in [2], but there Λ was set to 1 in the expansion. Since it is closely related to the volume of our map by (43), I would rather keep it. The differential equation (54) with $\Lambda = 1$ was solved by

$$\mathcal{F}_{\Lambda=1}(r) = \frac{3}{\sinh^2\left(\sqrt{\frac{3}{2}}r\right)}.$$

It is easy to check that this equation already obeys the necessary boundary conditions for our function $\mathcal{F}(r)$, namely that its limits at the endpoints of our spectrum of r should be $\mathcal{F}(r=0) = \infty$ and $\mathcal{F}(r=\infty) = 0$. Therefore, let us now set our solution to something similar to this, and try to find the correct form by substituting it into the original differential equation. We set

$$\mathcal{F}_\Lambda(r) = \frac{A}{\sinh^2\left(\Lambda^t\sqrt{\frac{3}{2}}r\right)},$$

and try to find the constants A and t. Substituting this into (54), we find

$$\frac{3A\ \Lambda^{2t}}{\sinh^4\left(\Lambda^t\ \sqrt{\frac{3}{2}}r\right)}\left(2\cosh^2\left(\Lambda^t\ \sqrt{\frac{3}{2}}r\right)+1\right) - \frac{6A\ \Lambda^{1/2}}{\sinh^2\left(\Lambda^t\sqrt{\frac{3}{2}}r\right)} - \frac{3A^2}{\sinh^4\left(\Lambda^t\sqrt{\frac{3}{2}}r\right)}.$$

Using the trigonometric identity $\cosh^2(x) = 1+\sinh^2(x)$, we can compare the coefficients of $\sinh^{-2}\left(\Lambda^t\sqrt{\frac{3}{2}}r\right)$ and $\sinh^{-4}\left(\Lambda^t\sqrt{\frac{3}{2}}r\right)$, to obtain the *consistency equations*

$$9A\ \Lambda^{2t} = 3A^2;$$
$$6A\ \Lambda^{2t} = 6A\ \Lambda^{1/2},$$

from which we can conclude that in our solution we should have $t = 1/4$, and $A = 3\ \Lambda^{1/2}$. Substituting this into our *ansatz*, the continuum partition function for surfaces with two marked points at geodesic distance $\geq r$, $\mathcal{F}_\Lambda(r)$, takes its final form

$$\mathcal{F}_\Lambda(r) = \frac{3\ \Lambda^{1/2}}{\sinh^2\left(\Lambda^{1/4}\sqrt{\frac{3}{2}}r\right)}. \tag{55}$$

Now we recall equation (23), and fill in the expansion of (52). We find that

$$\mathcal{G}_\Lambda(r) = \lim_{\epsilon\to 0} \frac{1}{\epsilon^3 R_\infty} G_k(x) = \lim_{\epsilon\to 0} \frac{1}{\epsilon}\left(\mathcal{F}_\Lambda(r-\epsilon) - \mathcal{F}_\Lambda(r)\right) \equiv -\frac{d\mathcal{F}(r)}{dr}, \tag{56}$$

and conclude that the *partition function for surfaces with two marked points at geodesic distance* ***equal to*** r is easily computed by differentiating (55) with respect to r and putting a minus sign in front. This leads us to

$$\mathcal{G}_\Lambda(r) = -\frac{d\mathcal{F}_\Lambda(r)}{dr} = 3\sqrt{6}\,\Lambda^{3/4}\frac{\cosh\left(\Lambda^{1/4}\sqrt{\frac{3}{2}}r\right)}{\sinh^3\left(\Lambda^{1/4}\sqrt{\frac{3}{2}}r\right)}. \tag{57}$$

This is precisely the form of the continuum partition function that was obtained in [1], in the context of *triangulations*. The fact that we have obtained the same form, is only displaying our hypothesis on the continuum two point function of discrete surfaces: up to constant rescaling, it *should* have the same form, no matter the building blocks of the surface!

3.3.4 Scale Invariance of the Continuum Two Point Function

Now that we have determined the form of the continuum partition function via an explicit calculation, we are interested in the scaling properties of the geodesic distance r as a function of the volume V. According to the rescaling of the graph distance in the *Brownian Map* by a factor $n^{1/4}$, it is natural to expect $\langle r\rangle$ to scale with $V^{1/4}$.
To be slightly more precise, we wish to show the *scale invariance* of the function $\mathcal{G}_V(r)$. This means that up to scalar multiplication the partition function $\mathcal{G}$ within the volume xV of the continuum variable r, should coincide with the function $\mathcal{G}$ within the volume V of the rescaled continuum variable $x^{-1/4}\,r$, for any $x \in \mathbb{R}_{\geq 0}$ - i.e.

$$\mathcal{G}_{xV}(r) = x^\alpha\,\mathcal{G}_V\left(x^{-1/4}\,r\right). \tag{58}$$

Firstly, let us calculate that this would indeed imply $\langle r\rangle_V = cV^{1/4}$. The expectation value of r is defined as

$$\langle r\rangle_V = \frac{\int_0^\infty r\,\mathcal{G}_V(r)\,dr}{\int_0^\infty \mathcal{G}_V(r)\,dr}. \tag{59}$$

Now, we note that equation (58) evaluated at $x = V^{-1}$ yields

$$\mathcal{G}_{xV}(r)|_{x=V^{-1}} = \mathcal{G}_1(r) = V^{-\alpha}\,\mathcal{G}_V\left(V^{1/4}r\right). \tag{60}$$

Upon making the substitution $V^{1/4}r \to r$, we find that

$$\mathcal{G}_V(r) = V^\alpha\,\mathcal{G}_1\left(V^{-1/4}r\right) \tag{61}$$

Plugging this into equation (59), and immediately making the reverse substitution $r \to V^{1/4}r$, we obtain

$$\langle r\rangle_V = \frac{\int_0^\infty V^\alpha\, rV^{1/4}\,\mathcal{G}_1(r)\,V^{1/4}dr}{\int_0^\infty V^\alpha\,\mathcal{G}_1(r)\,V^{1/4}dr} \tag{62}$$

$$= \langle r\rangle_1\,V^{1/4}, \tag{63}$$

where $\langle r\rangle_1$ is a well-defined constant, from which we can see that indeed $\langle r\rangle_V = cV^{1/4}$. However, in the previous section we have computed the continuum partition function $\mathcal{G}_\Lambda(r)$ instead of $\mathcal{G}_V(r)$. Luckily, we can rewrite the scale invariance of $\mathcal{G}_V(r)$ as a scale invariance requirement on $\mathcal{G}_\Lambda(r)$ as well - via the Laplace transform of equation (50) - and explicitly calculate that it does indeed hold for our form of the continuum partition

function (57).
To that end, let us write (according to equation (50))

$$\mathcal{G}_{x\Lambda}(r) = \int_0^\infty dV\ \mathcal{G}_V(r)\ e^{-x\Lambda V}. \tag{64}$$

Upon performing the substitution $xV \to V$, we find

$$\mathcal{G}_{x\Lambda}(r) = \int_0^\infty x^{-1} dV\ \mathcal{G}_{x^{-1}V}(r)\ e^{-\Lambda V}, \tag{65}$$

and finally using the scaling invariance of $\mathcal{G}_{x^{-1}V}(r)$ of equation (58), we find that the corresponding requirement on $\mathcal{G}_\Lambda(r)$ is given by

$$\mathcal{G}_{x\Lambda}(r) = x^{-1-\alpha} \int_0^\infty dV\ \mathcal{G}_V\left(x^{1/4} r\right)\ e^{-\Lambda V} = x^{-1-\alpha}\ \mathcal{G}_\Lambda\left(x^{1/4} r\right). \tag{66}$$

Computing $\mathcal{G}_{x\Lambda}(r)$ for the continuum partition function of equation (57), we find straightforwardly:

$$\mathcal{G}_{x\Lambda}(r) = 3\sqrt{6}\ \left(x\Lambda^{3/4}\right) \frac{\cosh\left(\left(x\Lambda^{1/4}\right)\sqrt{\frac{3}{2}} r\right)}{\sinh^3\left(\left(x\Lambda^{1/4}\right)\sqrt{\frac{3}{2}} r\right)} = x^{3/4}\ \mathcal{G}_\Lambda\left(x^{1/4} r\right) \tag{67}$$

and from this we can clearly see that the requirement of (66) is fulfilled for $\alpha = -7/4$. We can finally conclude that the continuum partition function (57) is indeed scale invariant, in the sense of (58). Therefore, we can conclude that this two point function obeys $\langle r \rangle_V = c V^{1/4}$. Since we defined our total volume as $V = n\epsilon^4$ (42), and our continuum scaling variable r as $r = k\epsilon$ (49), it follows that, in the limit $\epsilon \to 0$ and subsequently $n \to \infty$,

$$\langle k \rangle\ \epsilon = \langle r \rangle \propto V^{1/4} = n^{1/4}\ \epsilon \Rightarrow \langle k \rangle \propto n^{1/4}, \tag{68}$$

where we remember that k is the graph distance between two marked points. In this continuum limit, we find precisely the graph distance rescaling by a factor of $n^{1/4}$ according to the definition of the *Brownian Map* (1). Wonderful!

4 Eulerian Quadrangulations

The following section is on the more complex case of Eulerian quadrangulations. We will investigate a bijection between this class of maps and the class of trees called *labelled mobiles*, which will turn out to be slightly more difficult to enumerate than the well-labelled trees of the previous section. However, we will try our best to apply the same strategies as in the previous section to obtain a recursion relation for its generating function. From there on, we will see how the previous case of regular quadrangulations might help us out.

4.1 The Bouttier - Di Francesco - Guitter Bijection

First of all, it might be useful to state exactly what a Eulerian quadrangulation is.

Definition 4.1. A *Eulerian* quadrangulation is a bicolored quadrangulation of the plane, such that only faces of different colors are incident to each other.

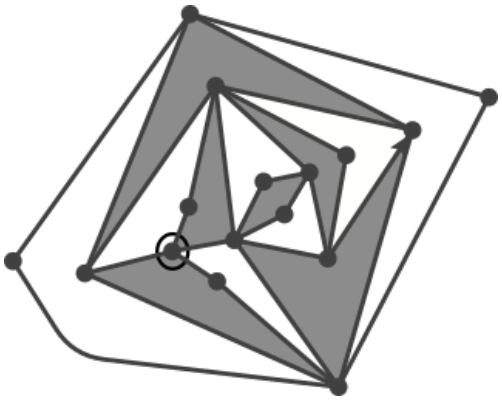

Figure 18: A pointed and rooted Eulerian quadrangulation. Note that in this figure, the outer face is black.

See figure 18 for an example. This is the example that will be used for the construction of our labelled mobile. For personal reasons - shortly mentioned in the introduction of this thesis - I will stick to the colors black and white. Following the *Schaeffer bijection* of section 3.1, we will now take a closer look at the *Bouttier - Di Francesco - Guitter* bijection for Eulerian quadrangulations. Originally, this bijection was designed for the much more general case of Eulerian maps; it takes on a drastic simplification in our case of quadrangulations.
Similar to the previous section on regular quadrangulations, let us define the class of trees that we are interested in. I have specified this definition to our case of Eulerian quadrangulations; for general Eulerian maps, the corresponding labelled mobiles need some additional information from the Eulerian maps [3], which is not necessary in our case.

Definition 4.2. A *labelled mobile* is a plane tree, such that:

1. Its vertices are of three types: unlabelled white vertices, unlabelled black vertices and labelled black vertices;

2. We have two types of edges: edges connecting labelled black vertices to unlabelled white vertices, and edges connecting unlabelled black vertices to unlabelled white vertices. Any white vertex has only one unlabelled black vertex attached;

3. All labels are positive integers and there is at least one vertex labelled 1;

4. Walking in counter-clockwise direction around a white vertex, starting from the attached unlabelled black vertex, the labels of the vertices must obey $n \to n+1 \to ... \to n+p-2$ before returning to the unlabelled black vertex, if the white vertex has degree p. It should be noted that in our case of quadrangulations, the white vertices have degree 4, and the walk will be: black unlabelled vertex $\to n \to n+1 \to n+2 \to$ black unlabelled vertex.

Let us now dive into the bijection.

Theorem 4.3. ***The Bouttier - Di Francesco - Guitter bijection.*** *There exists a bijection between rooted and pointed Eulerian quadrangulations and rooted labelled mobiles.*

Let us denote the set of Eulerian quadrangulations by $\mathcal{E}$, and the set of labelled mobiles by $\mathcal{M}$.

4.1.1 Construction: Labelled Mobile out of Eulerian Quadrangulation

We start with the construction $\Psi : \mathcal{E} \to \mathcal{M}$ of a labelled mobile $M \in \mathcal{M}$ out of a Eulerian quadrangulation $E \in \mathcal{E}$.

1. For the construction of M, we start with the rooted and pointed Eulerian quadrangulation of figure 18.
   The first step is already a tiny deviation from the procedure of section 3.1. We now impose the condition that we can only walk around the white faces in *counter-clockwise* order and around the black faces in *clockwise* order. While doing so, we label them with their 'asymmetric' geodesic distance from the pointed vertex. Furthermore, we require the root edge of E to be oriented according to the orientation that it obtains in this way.

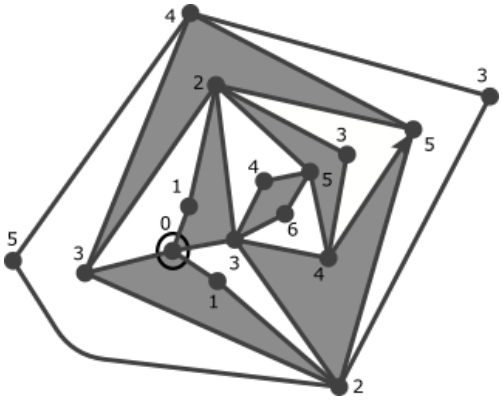

Figure 19: A Eulerian quadrangulation E with the vertices labelled according to their asymmetric geodesic distance.

2. After completing this step, we insert a new unlabelled vertex in every face of E with the color of the face it lies in. Subsequently, we draw edges in each face of E according to figure 20. This will automatically make sure that the resulting graph is connected, and is indeed a tree.

3. And finally, after erasing the original edges of E, we are left with the rooted *labelled mobile* M of figure 22. This completes the construction.

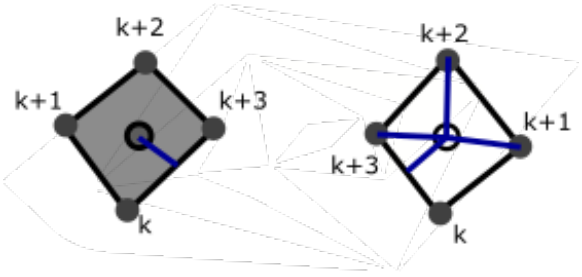

Figure 20: The selection rules.

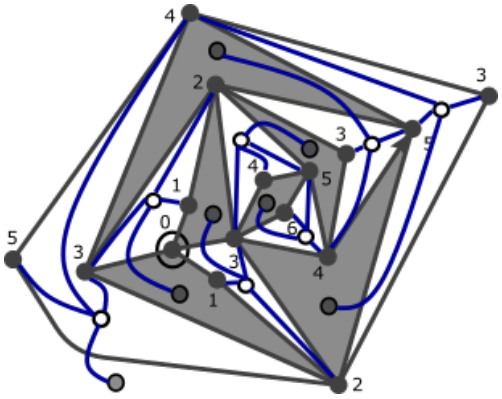

Figure 21: The edges of M are drawn according to figure 20.

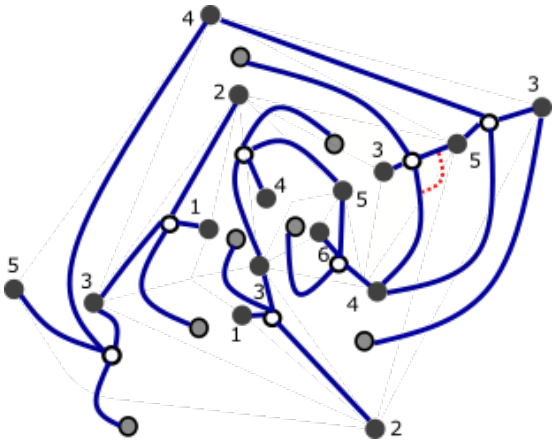

Figure 22: A labelled mobile.

4.1.2 Construction: Eulerian Quadrangulation out of Labelled Mobile

Even though the construction of section 4.1.1 is by far the most important for the remainder of this section, the least I can do to provide some insight as to why this would be a bijection, is to state the unique inverse construction $\Phi = \Psi^{-1} : \mathcal{M} \to \mathcal{E}$. However, for the sake of clarity, I will explain this construction using a slightly smaller labelled mobile than the one constructed in the previous section. To that end let us start with the pointed and rooted Eulerian quadrangulation of figure 23, and its corresponding rooted labelled mobile of figure 24.

Let us now turn to the construction.

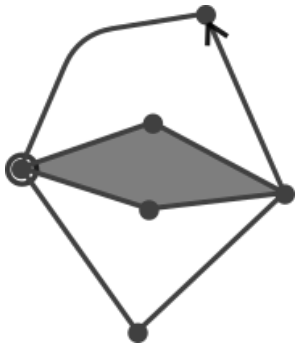

Figure 23: A Eulerian quadrangulation.

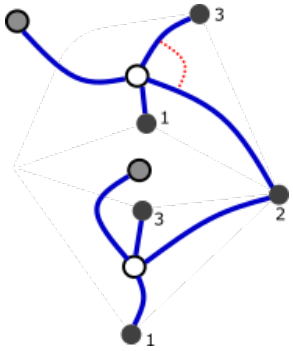

Figure 24: The labelled mobile corresponding to the Eulerian quadrangulation of figure 23.

1. We draw all the faces of the map according to the rules of figure 20. See figure 25. We label all the newly added vertices, since they only have one possible label from the construction rules.

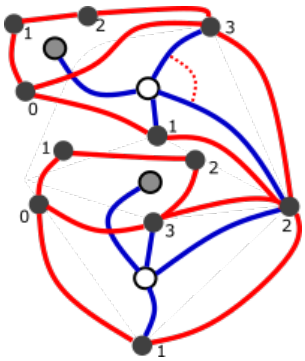

Figure 25: All the faces of the map drawn from the edges of the mobile.

2. Upon erasing all the original edges of the labelled mobile, we arrive at figure 26. Naturally, we keep all the original vertices of M, to indicate the color of the faces.

The edge that has now been drawn between the two vertices 'corresponding' to the root corner, becomes the new root edge of the map, with its orientation as prescribed by the first step of section 4.1.1.

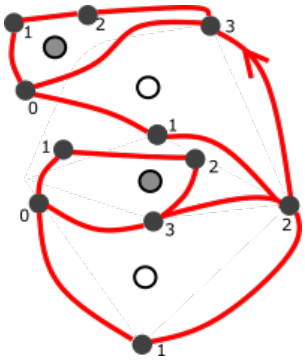

Figure 26: All the faces of the Eulerian quadrangulation, with the color as indicated by the vertex that lies in it. The root edge has been distinguished.

3. We observe that this map does indeed have as many faces as the original quadrangulation of figure 23, plus one outer face. Our task is now to correctly merge the edges of the map. Looking at figure 26, this is somehow quite intuitive. For a start, remember that we only want to merge edges that border black faces with edges that border white faces, and vice versa. Starting from the root of the associated mobile, we take walk around the contour of the map in clockwise direction. With this orientation, we 'associate' any edge of type $n \to n+1$ that borders a black face, with the next edge of type $n+1 \to n$ that we encounter on our clockwise walk, bordering a white face. All the edges around the black faces are of said type, since the edges that are of the type $n \to n-3$ have already been connected through our procedure of drawing the faces.
This is made visible in figure 27.

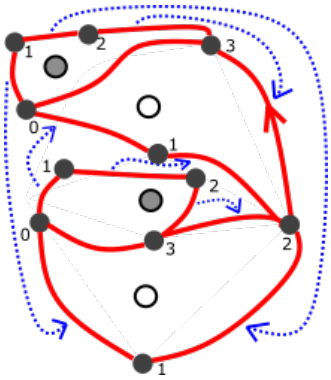

Figure 27: The matching procedure for the edges of the labelled mobile.

4. Now that we have a very clear correspondence between the edges bordering black and white faces respectively, the only thing that is left to do is to merge the associated edges. We color every face with the color of the vertex that lies in it. The vertex labelled '0' becomes the pointed vertex of the quadrangulation. This completes the construction. By construction the resulting map is the Eulerian

quadrangulation of figure 23.

Secondly, for the sake of completeness, let us show that we can recover the Eulerian quadrangulation of figure 18 from the labelled mobile of figure 22, by this procedure. This is shown in figures 28 - 31.

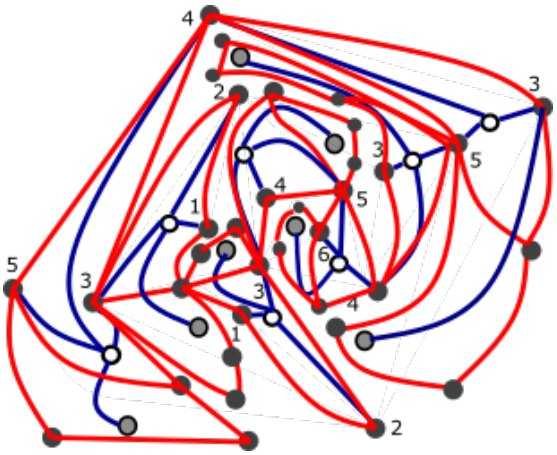

Figure 28: Drawing the faces of the quadrangulation from the selection rules.

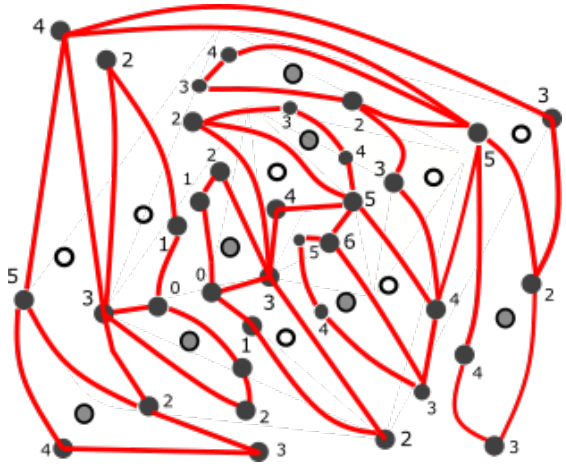

Figure 29: Labelling the vertices and deleting the original edges of the mobile.

For the more general cases of Eulerian maps and a thorough proof of the bijection, I would like to refer any interested reader to [3].
Now that we have succesfully established the bijection between rooted and pointed Eulerian quadrangulations and labelled mobiles, we are going to investigate how to obtain information on the scaling of distances within the quadrangulations from this bijection.

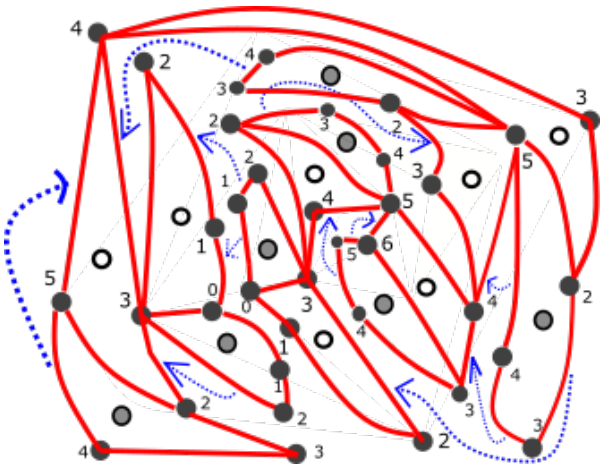

Figure 30: The matching of (some of) the edges according to the clockwise walk around the contour of the map.

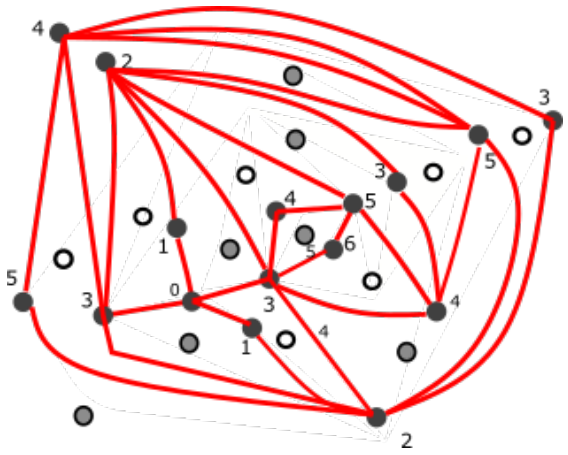

Figure 31: After contracting the edges, we are left with the Eulerian quadrangulation of figure 18.

4.2 Distances in Eulerian Quadrangulations: The Two Point Function

4.2.1 The Generating Function of Labelled Mobiles

Similar to the previous section, we will now investigate how to obtain a recurrence relation from the structure of the labelled mobiles. This task has become slightly more difficult now, since we are dealing with three different types of vertices instead of just one, and therefore we should distinguish between the types of edges going from a black to a white vertex and vice versa. Let us for clarity recall the labelled mobile that was constructed in section 4.1.1 - see figure 32. Firstly, it should be clear that we wish to obtain information on the distance between the *black vertices* of the mobile, since those are the ones that correspond to the original vertices of the Eulerian quadrangulation. One of the black vertices has naturally become the root of the tree, according to the procedure from 4.1.1: we have a distinguished edge, that is oriented towards the 'root vertex'. However, we have to note that the distance statistics we obtain from the

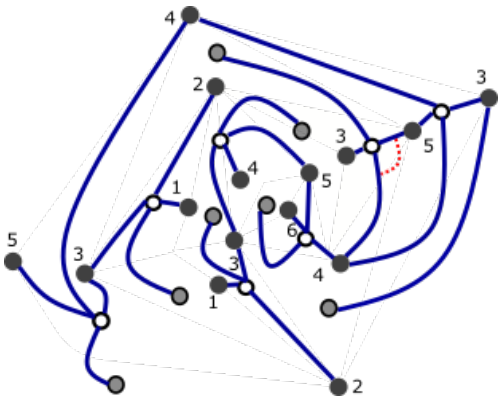

Figure 32: The labelled mobile from the previous section.

above bijection in this section, are in essence *asymmetric*, contrary to the symmetric distances of unicolored quadrangulations. This is because of the clockwise and counter-clockwise orientations of the edges around each black resp. white face of the Eulerian quadrangulation. In the end, we will see how to obtain information on *symmetric* distances within Eulerian quadrangulations, from the asymmetric distances we obtain using the Bouttier-di Francesco-Guitter bijection. For now, let us continue.
Similar to the previous section, we will establish a recursion for mobiles where the requirement that the minimal label be 1 is lifted. This will prove much more convenient to work with instead of general labelled mobiles, for the exact same reason as for regular quadrangulations - while constructing the recurrence relation, we will not have to worry about the actual values of the labels, and we will be able to translate this into an initial condition on the generating function.
Suppose we start from the black root vertex of an almost well-labelled mobile, labelled k, and denote the generating function of this root vertex going to a white vertex by $H_k(x)$. Again, this function also enumerates planar Eulerian quadrangulations of which the depth of the root edge is *at most* k. Taking a look at the possibilities for the tree to branch outwards from this root vertex, we see that it only has unlabelled white vertices attached, corresponding to the white faces, and it might have n of them. In section 3.1 we weighted the *edges* of the tree with x each, because those were the ones that corresponded to the faces of the original map. Here, it is therefore convenient to give only the white vertices weight x, since those are the ones that correspond to the white faces in the Eulerian quadrangulation. We will be able to define our volume only in terms of the white faces.
Let us denote the generating function of a white vertex going to a black vertex by $F_k(x)$, where this generating function inherits the label k from the black vertex it originates from. See the left side of figure 33.

This implies a relation between $H_k(x)$ and $F_k(x)$ given by

$$H_k(x) = \sum_{n=0}^{\infty} F_k^n(x) = \frac{1}{1 - F_k(x)}. \tag{69}$$

Say we arrived at a white vertex from a black vertex of label k. All white vertices have a total of 1 grey vertex (corresponding to the black faces of the quadrangulation) and 2 new(!) black vertices attached. The grey vertex is by construction always a *leaf*, which means that the tree does not continue from the grey vertex.
What might happen from here? To answer this question we make the following observation, already shortly mentioned in the definition of a *labelled mobile*. Denoting the

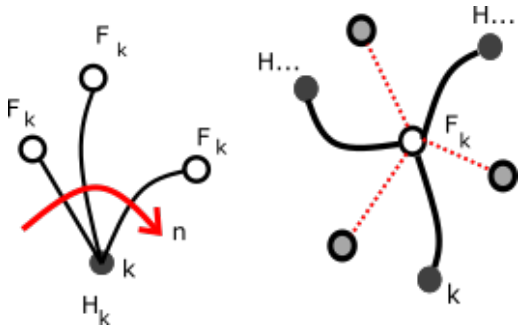

Figure 33: The branching possiblities for a labelled mobile corresponding to a Eulerian Quadrangulation.

minimal label of the three black vertices around a white vertex by p, the construction of the well-labelled mobile works in such a way that the order of the labels of the black vertices will be $p, p+1, p+2$, when going in counter-clockwise direction around the white vertex, starting from the only grey vertex it has attached. This can be explicitly checked to be true in the labelled mobile of figure 22. In essence, arriving at a white vertex 'with label k', the labels of the two black vertices it has attached strongly depend on the location of the black face in the Eulerian quadrangulation! This construction is summarized in the right side of figure 33. For example, it might be that k is the minimal label around the tree, in which case the only grey vertex should be directly to the left of this black vertex, and the other two black vertices have labels $k+1$ and $k+2$ consecutively. Taking the other two possibilities into account as well, and giving the white vertices weight x, we find the relation

$$F_k(x) = x\left(H_{k+1}(x)H_{k+2}(x) + H_{k+1}(x)H_{k-1}(x) + H_{k-1}(x)H_{k-2}(x)\right) \tag{70}$$

Combining (70) with (69) and rewriting, we find a recurrence relation on the generating function $H_k(x)$ of the form

$$H_k(x) = 1 + xH_k(x)\left(H_{k+1}(x)H_{k+2}(x) + H_{k+1}(x)H_{k-1}(x) + H_{k-1}(x)H_{k-2}(x)\right). \tag{71}$$

Comparing to the recursion of the generating function of regular quadrangulations, this is easily seen to be slightly messier. Solving this equation analytically is quite a stretch and slightly outside the scope of this thesis - even though it can be done [5]. Therefore, we will dive straight into the continuum limit approach, similar to section 3.3.3.

4.2.2 Critical Scaling

To start off, let us look at what happens in the limit where $k \to \infty$. Equation (71) reduces to

$$\lim_{k\to\infty} H_k(x) = H_\infty = 1 + 3xH_\infty^3. \tag{72}$$

This looks similar to (29), where we could immediately solve the quadratic equation and extract critical values. However, having the third power of H_∞ instead of the second power makes this very difficult to solve in a similar manner. Luckily, we do not necessarily need an exact solution in order to extract critical values.
Recalling that the value x_c corresponds to the radius of convergence of the generating function H_∞, finding the critical value x_c corresponds to finding the first singularity of

the function $H_\infty(x)$ on the real x-axis. This is equivalent to finding the first *stationary point* of the inverse function $x\left(H_\infty\right)$. Inverting equation (72), we find

$$x\left(H_\infty\right) = \frac{H_\infty - 1}{3H_\infty^3}. \tag{73}$$

Subsequently setting the derivative of this equation with respect to H_∞ to zero, we find the value of H_∞ at the critical point x_c to be

$$\frac{d}{dH_\infty}\left(\frac{H_\infty - 1}{3H_\infty^3}\right) = \frac{1}{H_\infty^4} - \frac{2}{3H_\infty^3} = 0 \rightarrow H_\infty(x_c) = \frac{3}{2}. \tag{74}$$

From this we can immediately extract the critical value x_c itself, and we find that it is given by

$$x_c = \frac{H_\infty(x_c) - 1}{3H_\infty(x_c)} = \frac{3/2 - 1}{3 \cdot (3/2)^3} = \frac{4}{81}. \tag{75}$$

Furthermore, this singularity analysis allows us to determine the asymptotic growth of the coefficients, from theorem 3.9. Expanding $x(H_\infty)$ around its critical point $H_\infty(x_c)$, we find

$$\begin{aligned} x(H_\infty) \approx \frac{H_\infty(x_c) - 1}{{H_\infty}^3(x_c)} &+ \left(\frac{1}{H_\infty^4(x_c)} - \frac{2}{3H_\infty^3(x_c)}\right)\left(H_\infty(x) - H_\infty(x_c)\right) \\ &+ \frac{1}{2}\left(\frac{2}{H_\infty^4(x_c)} - \frac{4}{H_\infty^5(x_c)}\right)\left(H_\infty(x) - H_\infty(x_c)\right)^2 + ... \end{aligned}$$

However, our critical value x_c is defined such that the derivative of the function $x(H_\infty)$ would vanish at x_c. Therefore, the first singularity of $x(H_\infty)$ is of the form $\left(H_\infty(x) - H_\infty(x_c)\right)^2$, from which we can conclude that the first singularity of the inverse $H_\infty(x)$ indeed has the same square root singularity as regular quadrangulations. Its coefficients grow asymptotically as (40). Furthermore, let us quickly calculate the value of $x_c H_\infty^2$,

$$x_c H_\infty(x_c)^2 = \frac{3/2 - 1}{3 \cdot 3/2} = \frac{1}{9}, \tag{76}$$

since this will prove to be useful later on.
Now that all of this is settled, we can finally continue our quest to find the appropriate scaling for Eulerian quadrangulations. To that end, we let x tend to its critical value x_c by

$$x = x_c\left(1 - \Lambda\epsilon^4\right) = \frac{4}{81}\left(1 - \Lambda\epsilon^4\right), \tag{77}$$

and define our total volume (identical to (42)), as

$$V = n\epsilon^4. \tag{78}$$

In this case, we have to once again remind ourselves that only the *white faces* have been weighted by x. Therefore, the number n corresponds to the number of white faces of the map. Since the map is - of course - connected, this will not make a difference when considering (asymmetric) geodesic distances, and in the large n limit it is convenient to define the volume only in terms of the white faces.
Similar to (49), we rewrite our geodesic distance k in terms of a *continuum scaling variable* r as

$$k \equiv \frac{\gamma r}{\epsilon}. \tag{79}$$

Furthermore, we expand our recursion relation in terms of a *yet to be determined* continuum partition function $\mathcal{F}$, as in (52), by

$$H_k = H_\infty\left(1 - \beta\epsilon^2\mathcal{F}(k\epsilon/\gamma)\right). \tag{80}$$

To summarize - our goal is to show that for a certain choice of constants γ and β, the form of the two point function for Eulerian quadrangulations will reduce to that of regular quadrangulations. This would mean that - up to global scalar multiplication - the scaling laws for the two models are the same!
The following calculation will be a bit tedious, but it is necessary. Substituting (80) into (71), we obtain

$$\begin{aligned}H_\infty(1-\beta\epsilon^2\mathcal{F}(k\epsilon/\gamma) = 1 + xH_\infty^3(1-\beta\epsilon^2\mathcal{F}(k\epsilon/\gamma)((1-\beta\epsilon^2\mathcal{F}((k\epsilon+2\epsilon)/\gamma))(1-\beta\epsilon^2\mathcal{F}((k\epsilon+\epsilon)/\gamma))\\ + (1-\beta\epsilon^2\mathcal{F}((k\epsilon+\epsilon)/\gamma))(1-\beta\epsilon^2\mathcal{F}((k\epsilon-\epsilon)/\gamma))\\ + (1-\beta\epsilon^2\mathcal{F}((k\epsilon-2\epsilon)/\gamma))(1-\beta\epsilon^2\mathcal{F}((k\epsilon-\epsilon)/\gamma))).\end{aligned}$$

Now, let us again expand this up to fourth order in ϵ and separate the different powers. We compute straightforwardly

$$\mathcal{O}(1) : H_\infty = 1 + 3xH_\infty^3$$

$$\begin{aligned}\mathcal{O}(\epsilon^2) : -\epsilon^2\beta xH_\infty\mathcal{F}(r) = -3\epsilon^2\beta xH_\infty^3\mathcal{F}(r)\\ -\epsilon^2\beta xH_\infty^3\left(\mathcal{F}(r+2\epsilon/\gamma) + 2\mathcal{F}(r+\epsilon/\gamma) + 2\mathcal{F}(r-\epsilon/\gamma) + \mathcal{F}(r-2\epsilon/\gamma)\right)\end{aligned}$$

$$\begin{aligned}\mathcal{O}(\epsilon^4) : 0 = \epsilon^4\beta^2xH_\infty^3\mathcal{F}(r)\left(\mathcal{F}(r+2\epsilon/\gamma) + 2\mathcal{F}(r+\epsilon/\gamma) + 2\mathcal{F}(r-\epsilon/\gamma) + \mathcal{F}(r-2\epsilon/\gamma)\right)\\ +\epsilon^4\beta^2xH_\infty^3\left(\mathcal{F}(r+2\epsilon/\gamma)\mathcal{F}(r+\epsilon/\gamma) + \mathcal{F}(r+\epsilon/\gamma)\mathcal{F}(r-\epsilon/\gamma) + \mathcal{F}(r-\epsilon/\gamma)\mathcal{F}(r-2\epsilon/\gamma)\right).\end{aligned}$$

Let us try to organize this 'mess' by dividing through H_∞, and again taking all the ϵ^2-terms to the left side and the ϵ^4-terms to the right side, as we remember that in the original equation the terms were part of one and the same equation and should be added up in the end. We obtain

$$\epsilon^2\left(3\beta xH_\infty^2\mathcal{F}(r) - \beta\mathcal{F}(r) + \beta xH_\infty^2\left(\mathcal{F}(r+2\epsilon/\gamma) + 2\mathcal{F}(r+\epsilon/\gamma) + 2\mathcal{F}(r-\epsilon/\gamma) + \mathcal{F}(r-2\epsilon/\gamma)\right)\right)$$

$$\begin{aligned}= \epsilon^4(\beta^2xH_\infty^2(\mathcal{F}(r)\mathcal{F}(r+2\epsilon/\gamma) + 2\mathcal{F}(r)\mathcal{F}(r+\epsilon/\gamma) + 2\mathcal{F}(r)\mathcal{F}(r-\epsilon/\gamma) +\\ \mathcal{F}(r)\mathcal{F}(r-2\epsilon/\gamma) + \mathcal{F}(r+2\epsilon/\gamma)\mathcal{F}(r+\epsilon/\gamma) + \mathcal{F}(r+\epsilon/\gamma)\mathcal{F}(r-\epsilon/\gamma) +\\ \mathcal{F}(r-\epsilon/\gamma)\mathcal{F}(r-2\epsilon/\gamma))) + \mathcal{O}(\epsilon^6).\end{aligned}$$

Following our discussion on the critical values of H_∞, we can now let x tend to its critical value, which corresponds to making the substitution $xH_\infty^2 \to \frac{1}{9}(1-\Lambda^{1/2}\epsilon^2)$, similar to equation (46). Then, multiplying left and right by a factor of 9 and once more expanding the equation up to order ϵ^4, this yields

$$\epsilon^2\left(3\beta\mathcal{F}(r) - 9\beta\mathcal{F}(r) + \beta(\mathcal{F}((r+2\epsilon/\gamma) + 2\mathcal{F}((r+\epsilon/\gamma) + 2\mathcal{F}(r-\epsilon/\gamma) + \mathcal{F}(r-2\epsilon/\gamma)))\right.$$

$$\begin{aligned}= \epsilon^4\left(3\beta\Lambda^{1/2}\mathcal{F}(r) + \beta\Lambda^{1/2}(\mathcal{F}(r+2\epsilon/\gamma) + 2\mathcal{F}(r+\epsilon/\gamma) + 2\mathcal{F}(r-\epsilon/\gamma) + \mathcal{F}(r-2\epsilon/\gamma))\right.\\ +\beta^2(\mathcal{F}(r)\mathcal{F}(r+2\epsilon/\gamma) + 2\mathcal{F}(r)\mathcal{F}(r+\epsilon/\gamma) + 2\mathcal{F}(r)\mathcal{F}(r-\epsilon/\gamma) +\\ \mathcal{F}(r)\mathcal{F}(r-2\epsilon/\gamma) + \mathcal{F}(r+2\epsilon/\gamma)\mathcal{F}(r+\epsilon/\gamma) + \mathcal{F}(r+\epsilon/\gamma)\mathcal{F}(r-\epsilon/\gamma) +\\ \mathcal{F}(r-\epsilon/\gamma)\mathcal{F}(r-2\epsilon/\gamma))) + \mathcal{O}(\epsilon^6).\end{aligned}$$

Dividing by $\beta\epsilon^4$, and taking the desired limit $\epsilon \to 0$, we *finally*(!) find

$$\begin{aligned}\lim_{\epsilon\to 0}\left(\frac{1}{\epsilon^2}(\mathcal{F}(r+2\epsilon/\gamma) - 2\mathcal{F}(r) + \mathcal{F}(r-2\epsilon/\gamma) + 2\mathcal{F}(r+\epsilon/\gamma) - 4\mathcal{F}(r) + 2\mathcal{F}(r+\epsilon/\gamma))\right)\\ = 3\Lambda^{1/2}\,\mathcal{F}(r) + 6\Lambda^{1/2}\,\mathcal{F}(r) + 9\beta\mathcal{F}^2(r) + \mathcal{O}(\epsilon^2).\end{aligned}$$

Again, using the definition of the second derivative (twice!), we obtain

$$\frac{6}{\gamma^2}\frac{d^2\mathcal{F}(r)}{dr^2} = 9\Lambda^{1/2}\ \mathcal{F}(r) + 9\beta\mathcal{F}^2(r), \tag{81}$$

and upon multiplying by $2/3$ and rearranging the terms, we find the following final form of the differential equation for our continuum partition function $\mathcal{F}(r)$, given by

$$\frac{4}{\gamma^2}\frac{d^2\mathcal{F}(r)}{dr^2} - 6\Lambda^{1/2}\ \mathcal{F}(r) - 6\beta\mathcal{F}^2(r) = 0. \tag{82}$$

We see that upon choosing the values $\gamma = 2$ and $\beta = 1/2$, this gives us the exact same differential equation as for the regular quadrangulations (54)!
This means that, up to constant rescaling of the partition function $\mathcal{F}(k\epsilon/\gamma)$ of two marked points at 'continuum' geodesic distance $\geq r$ by a factor of $1/2$, and constant rescaling of our definition of the geodesic graph distance k by a factor of 2, we can obtain this partition function for the case of regular quadrangulations out of the partition function for Eulerian quadrangulations. From this we can similarly extract the partition function for geodesic distances *equal to* r by differentiating $\mathcal{F}(r)$ with respect to r, which automatically implies that it does indeed obey the same scale invariance law (58) as before! Furthermore, we still have

$$k \propto r/\epsilon,\ \langle r\rangle \propto V^{1/4} \to \langle k\rangle \propto n^{1/4} \tag{83}$$

where n corresponds to the number of white squares in the Eulerian quadrangulation, since those are the faces that were weighted in the our recursion, and the total volume is defined as in (78). Furthermore, from the exactly computed values of $\gamma = 2$ and $\beta = 1/2$, we can deduce for the relation between the graph distances $\langle k^Q\rangle$ and $\langle k^{EQ}\rangle$ for quadrangulations and Eulerian quadrangulations respectively (where we have to remember that the graph distances k^{EQ} are still with respect to their orientation!), that

$$\langle k^Q\rangle_n = 1/2\ \langle k^{EQ}\rangle_{2n} = 2^{-3/4}\langle k^{EQ}\rangle_n, \tag{84}$$

where the factor of $1/2$ comes from γ, because upon multiplying our scaling law by $1/2$, we go from 'Eulerian' distances to 'regular' distances. The factor of 2 in front of the number of squares n comes from β, since β tells us something about the ratio between the number of regular and Eulerian quadrangulations in the limit of very large n.
Furthermore, we can give a lower and an upper bound on the symmetric graph distance within Eulerian quadrangulations, in terms of the asymmetric graph distance. The largest asymmetric distance that two points at geodesic distance k might have is given by $3k$, because the asymmetric graph distance and the graph distance maximally differ by a factor of 3 across each face of the quadrangulation. Similarly, the smallest distance they might have is just given by k. Therefore we may write that

$$\frac{1}{3}d^{EQ}_{gr} \leq d^{Q}_{gr} \leq d^{EQ}_{gr}, \tag{85}$$

which readily shows that also the symmetric graph distance within Eulerian quadrangulations, up to scalar multiplication, scales with the usual power of $n^{1/4}$ in the large n limit.

5 Discussion

In this thesis, we have seen two different bijections between maps and trees. In the introduction, we set our goal to show that the universality of the Brownian Map (1) extends to *bicolored* quadrangulations as well as regular quadangulations (and all other p-angulations, for that matter). We have thoroughly examined the case of regular quadrangulations via their bijection with well-labelled trees. Firstly, I tried to give a more intuitive explanation of this rescaling factor of one fourth, using the properties of random walks on the trees and their labels. Secondly, we have seen a derivation of this scaling limit, by solving the recursion relation for the generating function of well-labelled trees and deriving its Continuum Two Point Function. From there we saw, via an explicit calculation, that indeed in this continuum limit geodesic distances scale with the fourth root of the total volume of the map.

Subsequently we tried to extend this to the case of bicolored or *Eulerian* quadrangulations. A bijection between Eulerian quadrangulations and labelled mobiles was established, thanks to the work of Bouttier, di Francesco and Guitter [3]. This time it proved slightly more complicated to solve the recurrence relation for these mobiles exactly, but by singularity analysis we were able to establish the critical values of the generating function. We used these to expand the generating function in the continuum limit, and explicitly showed that for a certain choice of parameters we may obtain the Continuum Two Point Function for regular quadrangulations out of the one for Eulerian quadrangulations. Therefore we established that up to scalar multiplication of our definition of *geodesic distance*, and of the Two Point Function itself, the distributions for the two families of quadrangulations are equal and the scaling limits indeed do coincide. Though it is not a proof, at least is a great indication that Eulerian quadrangulations are within the universality class of the Brownian Map.

As shortly stated in the introduction, this thesis was on two dimensional quantum gravity *without matter* - we have only considered the geometry of spacetime itself, and derived the scaling limit for two discrete models. However, Eulerian maps, such as the quadrangulations of section 4, can be of great use when matter is involved. General maps where matter is included, such as the Ising model or similar models of interacting particles, can be nicely translated to the study of Eulerian maps, with some additional constraints. One can e.g. characterize such models by blocking certain edges of the quadrangulation, or putting restrictions on the total number of particles that is allowed between adjacent faces of Eulerian maps, as in [4]. Using techniques shown in this article, one can come up with recursive equations for the generating functions of such systems, which may be analyzed in the limit of large n, as we have seen for the case where matter is absent. □.

- -

References

[1] J. Ambjørn and Y. Watabiki. Scaling in quantum gravity. *Nuclear Physics B*, 445:129–142, 1995.

[2] J. Bouttier, P. Di Francesco, and E. Guitter. Geodesic Distance in Planar Maps. *Nuclear Physics B*, 663:535–567, 2003.

[3] J. Bouttier, P. Di Francesco, and E. Guitter. Planar maps as labeled mobiles. *The Electronic Journal of Combinatorics*, 11, 2004.

[4] J. Bouttier, P. Di Francesco, and E. Guitter. Blocked edges on Eulerian maps and mobiles: Application to spanning trees, hard particles and the Ising model. *Journal of Physics A Mathematical and Theoretical*, 40:7411–7440, 2007.

[5] J. Bouttier, E. Fusy, and E. Guitter. On The Two-Point Function Of General Planar Maps and Hypermaps. *Annales de l'Institut Henri Poincaré D*, 1:265–306, 2014.

[6] R Chapman. Moments of Dyck Paths. *Discrete Mathematics*, 204:113 – 117, 1998.

[7] G. Chapuy. An introduction to map enumeration. 2014.

[8] P. Chassaing and G. Schaeffer. Random Planar Lattices and Integrated Superbrownian Excursion. *Probability Theory and Related Fields*, 128:161–212, 2004.

[9] T. Davis. Catalan Numbers. 2016.

[10] A. Ekart. The Cori-Vauquelin-Schaeffer Bijection and its Applications in the Theory of Scaling Limits of Random Labelled Quadrangulations and Trees. 2015.

[11] P. Flajolet and R. Sedgewick. *Analytic Combinatorics*. Cambridge University Press, 2009.

[12] I.M. Gessel. Lagrange Inversion.

[13] A. Perez. Determining the Genus Of a Graph. 2009.